

Review

Chitosan-Based Particulate Carriers: Structure, Production and Corresponding Controlled Release

Jiaqi Weng^{1,2}, Alain Durand²  and Stéphane Desobry^{1,*} ¹ Université de Lorraine, LIBio, F-54000 Nancy, France; jiaqi.weng@univ-lorraine.fr² Université de Lorraine, CNRS, LCPM, F-54000 Nancy, France; alain.durand@univ-lorraine.fr

* Correspondence: stephane.desobry@univ-lorraine.fr; Tel.: +33-(0)-3-72-74-40-96

Abstract: The state of the art in the use of chitosan (CS) for preparing particulate carriers for drug delivery applications is reviewed. After evidencing the scientific and commercial potentials of CS, the links between targeted controlled activity, the preparation process and the kinetics of release are detailed, focusing on two types of particulate carriers: matrix particles and capsules. More precisely, the relationship between the size/structure of CS-based particles as multifunctional delivery systems and drug release kinetics (models) is emphasized. The preparation method and conditions greatly influence particle structure and size, which affect release properties. Various techniques available for characterizing particle structural properties and size distribution are reviewed. CS particulate carriers with different structures can achieve various release patterns, including zero-order, multi-pulsed, and pulse-triggered. Mathematical models have an unavoidable role in understanding release mechanisms and their interrelationships. Moreover, models help identify the key structural characteristics, thus saving experimental time. Furthermore, by investigating the close relation between preparation process parameters and particulate structural characteristics as well as their effect on release properties, a novel “on-demand” strategy for the design of drug delivery devices may be developed. This reverse strategy involves designing the production process and the related particles’ structure based on the targeted release pattern.

Keywords: chitosan; controlled release; particles; capsules

check for updates

Citation: Weng, J.; Durand, A.; Desobry, S. Chitosan-Based Particulate Carriers: Structure, Production and Corresponding Controlled Release. *Pharmaceutics* **2023**, *15*, 1455. <https://doi.org/10.3390/pharmaceutics15051455>

Academic Editor: Barbara Stella

Received: 3 April 2023

Revised: 30 April 2023

Accepted: 4 May 2023

Published: 10 May 2023



Copyright: © 2023 by the authors. Licensee MDPI, Basel, Switzerland. This article is an open access article distributed under the terms and conditions of the Creative Commons Attribution (CC BY) license (<https://creativecommons.org/licenses/by/4.0/>).

1. Introduction

Chitosan (CS), derived from chitin through deacetylation, is a natural polymer with enormous potential applications in biotechnology and food engineering. Chitin is a long-chain polymer of N-acetyl glucosamine and the second most abundant natural biopolymer after cellulose on the planet [1–5]. The estimated annual biosynthesis of chitin is roughly 1010 tons in the biosphere [6]. It is a sustainable natural resource that is omnipresent but still underexploited commercially. Chitin and cellulose belong to the same class of biopolymers, i.e., polysaccharides. The two other main classes of biopolymers include proteins and nucleic acids.

CS is a linear polysaccharide composed of amino groups, with its structure containing D-glucosamine (deacetylated units) and N-acetyl-D-glucosamine (acetylated units) linked randomly through β -(1→4) bonds (Figure 1) [7]. Due to its repeatedly reported beneficial characteristics, such as the absence of toxicity, biocompatibility and biodegradability, CS has found considerable applications in various fields, including environmental engineering, agriculture, aquaculture, agrochemistry, the food industry and the medical/pharmaceutical and cosmetic industries [8–11].

Chitin can be extracted from algae, fungi, arthropods (crabs, shrimp, crayfish and insects), plankton and mollusks (squids). Nowadays, the main commercial sources of chitin and its derivatives are shells and the exoskeleton of crustaceans, which used to be considered low-value marine wastes. The global annual production of shrimp or

lobster shells and crab waste was reported to be between 6 and 8 million tons [12]. For instance, crustacean shells contain roughly 15–40 wt% of chitin [13]. The powder of this grounded marine byproduct can serve as an animal-feed supplement, but with very limited profitability compared with its refined, high-value chemicals (Table 1). The transformation of chitin from marine waste is not complex, but the process requires considerable amounts of water and chemical components such as strong acids and bases. Additionally, the final product quality varies a lot depending on the raw material (species of shellfish as well as types and quantities of impurities).

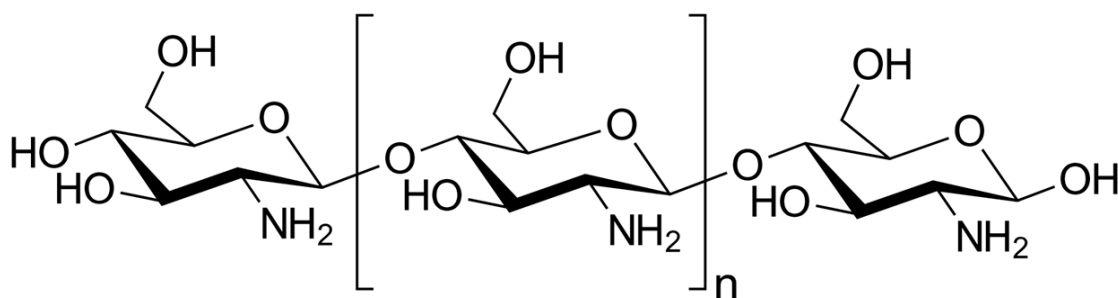


Figure 1. Chemical structure of chitosan from completely deacetylated chitin.

Table 1. Global annual production and price of chitin, chitosan and dried shrimp shells.

Product	Industrial Production (10 ⁶ Tons Per Year)	Price (USD Per Ton)
Dried shrimp shells	6–8	100–120 [14,15]
Chitin	0.02–0.04 ⁱ	6000–40,000
Chitosan	<0.2 ⁱⁱ	15,000–160,000 ⁱⁱⁱ

ⁱ Annual production of chitin is probably under 10,000 tons, whereas more recent figures are not available [14].

ⁱⁱ Global industrial production of chitosan is estimated to reach 173.9 thousand tons by 2027 [9]. ⁱⁱⁱ Data from Alibaba (March 2023) [16].

The industrial production of refined chitin/chitosan and their derivatives remained low by 2016. Indeed, it was reported that less than half of the global demand was satisfied [15,17]. Both demand and production for CS have kept growing in various industries worldwide during the last few years. The global market volume of chitin and its derivatives was valued at nearly USD 7.1 billion by 2021 [18], was estimated at USD 7.9 billion in 2022 and is foreseen to reach a revised size of USD 24.9 billion by 2030 [19].

1.1. Emerging Research and Industrial Interest for Chitosan

The first interest in commercializing chitin was held back in the 1930s because of the strong competition with synthesized polymers at that time. Large-scale production of chitin regained attention in the mid-1970s, when regulations aiming to reduce the dumping of shellfish waste were introduced. Regarding research interest, 108,025 references concerning “chitin/chitosan” were found using SciFinder (years between 1970 and 2022). A remarkable increase in the number of publications was evidenced at the beginning of the 1990s, indicating a real emerging research interest in the academic world (Figure 2). On the other hand, according to statistics from WIPO’s database, PATENTSCOPE, the potential commercial applications of CS have grown steadily since the late twentieth century, whereas the number of patent applications concerning CS has exploded in the last three decades. A total of 51,274 patent application records in English were found from all offices (Figure 3).

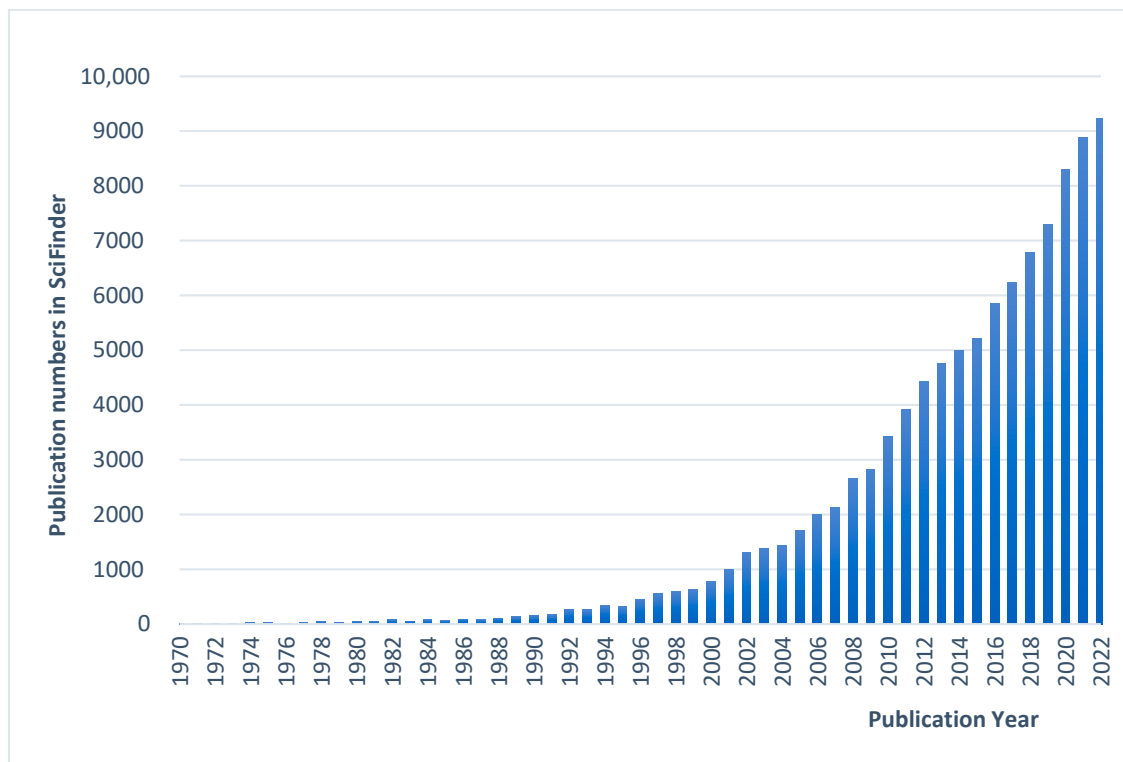


Figure 2. Number of publications containing the keywords “chitin” or “chitosan” registered each year in SciFinder. Books, conferences, editorials, journal articles, preprints and reviews included. (Data from SciFinder, March 2023).

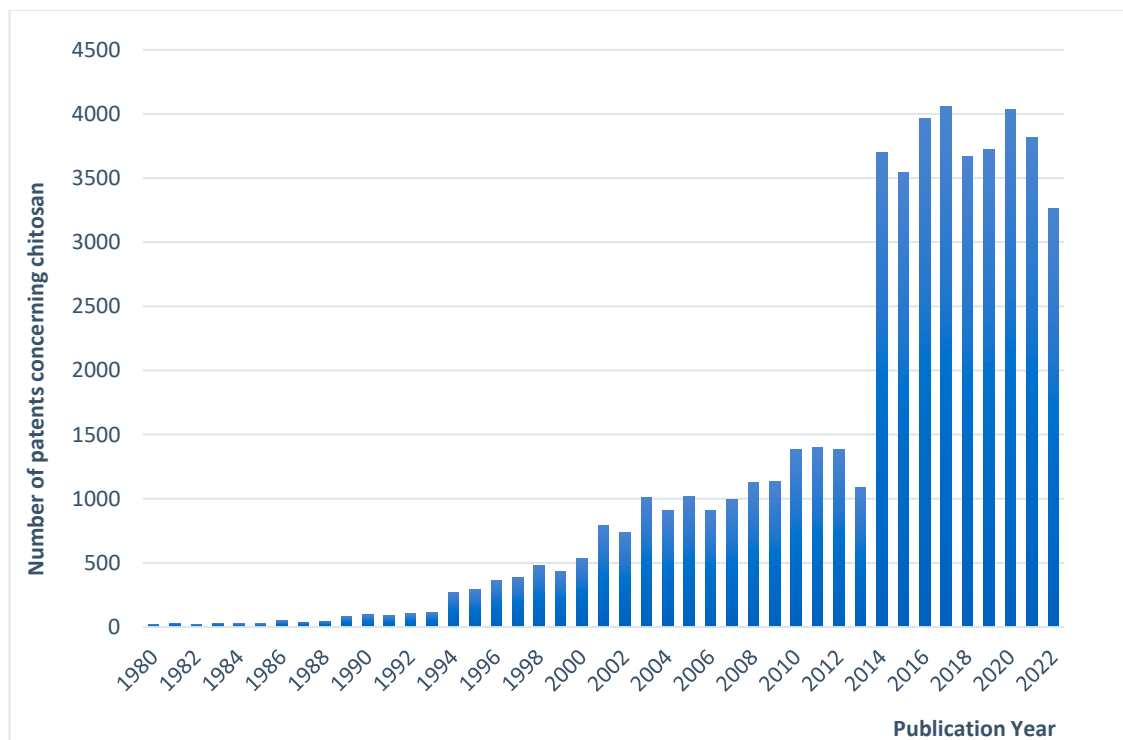


Figure 3. Number of patents relevant to the keywords “chitin” or “chitosan” in English published each year. (Data from WIPO, <https://patentscope.wipo.int/search/en/result.jsf/> (accessed on 1 March 2023)).

1.2. A Multiple-Application Biopolymer

Chitosan's multiple utilities originate from its relatively specific chemical and physical properties. Indeed, it is the unique example of a cationic polyelectrolyte among known natural polysaccharides. Thus, complexes, or coacervates, can be produced through electrostatic interactions between chitosan and other negatively charged compounds. Because of its beneficial biological properties, such as non-toxicity, biodegradability, biocompatibility, mucoadhesive behavior and antimicrobial activities, it is apt to bind with electronegative mucous membranes, and it shows low in vitro toxicity as well as in the case of some in vivo models [20]. CS is also a pH-sensitive material whose dissolution in water is possible only under mildly acidic conditions ($\text{pH} < 6.5$). This may sometimes be considered a limitation. CS derivatives with extended water solubility can be obtained through chemical modification of the chains, such as carboxymethylation, quaternization and hydroxypropylation [21]. There are many examples of functional groups that have been introduced onto the CS chain to form water-soluble derivatives [22], e.g., thiolated CS [23], glycol CS [24,25], quaternized CS [26], carboxymethyl CS [27], isobutyl CS [28] and oligoethylene oxide sulfonate CS [29]. In addition to its well-known applications in various fields (Figure 3), CS has significant potential for managing hyperlipidemia [30]. Recently, there have been reports on the beneficial effects of CS in controlling the COVID-19 pandemic [31,32]. To conclude, CS's availability (relying on abundant reserves in nature), benign properties and versatile applications rationalize the ongoing research enthusiasm from both academia and industry.

1.3. Terminology of Particulate Carriers

Due to chitosan's versatile properties mentioned above, its application as a delivery system has been reported in numerous papers. At the level of the particulate carrier, CS is commonly used as the principal polymer to build up the carrier's core material as well as the peripheral material to coat or/and impart novel functionality to the vector.

Within the scope of this review, particulate carriers are defined as micro- or nano-sized particulate dispersions of liquid or solid particles. The size range is first related to the route of administration. In addition, the nanometric size range endows this type of object with interesting properties as a delivery system because of the large specific area, which usually facilitates the release of active molecules. Alternatively, their surface is available for further functionalization, providing specific interaction properties potentially leading to targeting. Understanding and characterizing the nature/morphology/size of particles is important for designing and optimizing particle-based systems for specific applications (Figure 4). Additionally, a particle's shape can have a significant influence on its physical, chemical and biological properties, e.g., surface area, packing properties, flow behavior, mechanical properties, drug release kinetics and efficiency [33–36].

A complex nomenclature of particulate carriers exists in the literature [37,38]. Within the scope of this review, prefixes indicate the size of the carrier, such as micro-/nano-. Micro-/nanospheres refer to spherical particles with diameters in the micrometer/nanometer range (Figure 5). According to the International Union of Pure and Applied Chemistry (IUPAC), the lower limit between micro- and nano-sizing is still a matter of debate. This review adapted the terminology of IUPAC (Table 2). A nanoparticle refers to a particle of any shape with at least one dimension between 10^{-9} and 10^{-7} m. The upper limit is chosen as 100 nm because novel properties that distinguish particles from bulk material normally show up at a critical dimension scale lower than 100 nm [39]. Nevertheless, due to certain phenomena (transparency, ultrafiltration, stable dispersion, etc.), the upper limit can be acceptably extended up to 500 nm. Nanoparticles can be divided into two categories: homogeneous nanoparticles, also known as "nanospheres," and core-shell structured nanoparticles, known as "nanocapsules" (Figure 6) [40–43].

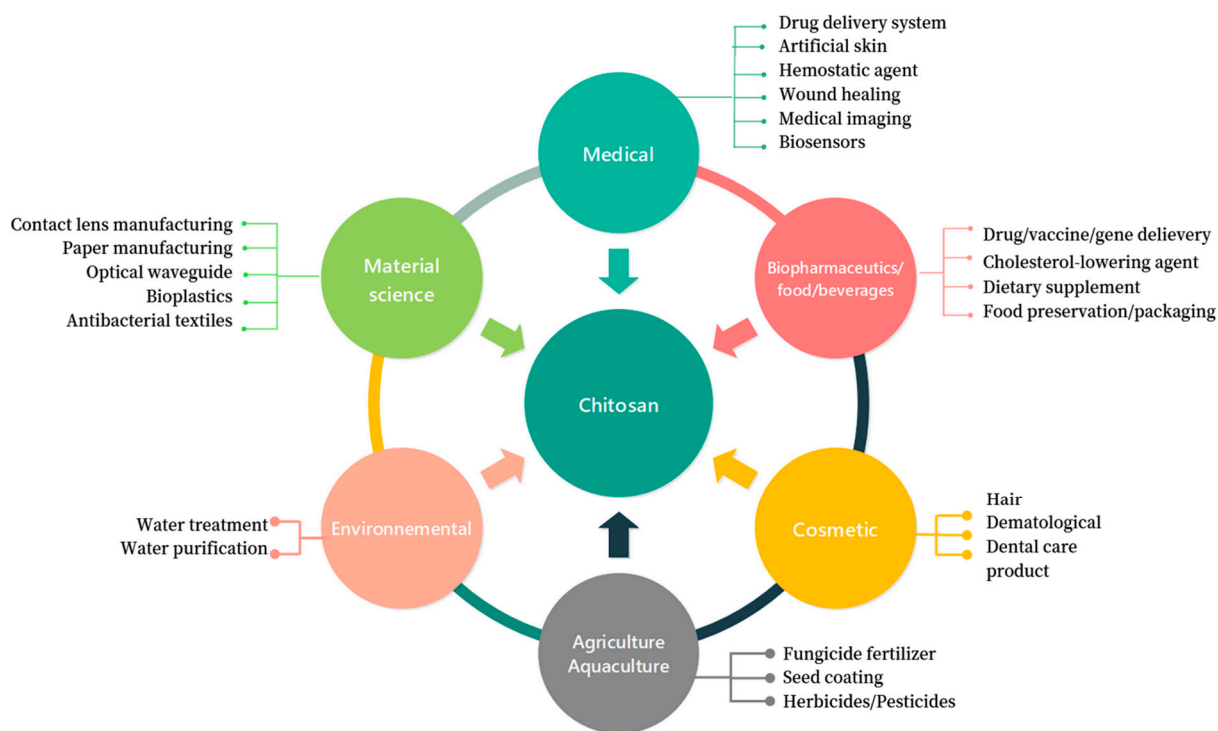


Figure 4. Schematic overview of the versatility of chitosan applications in various fields.

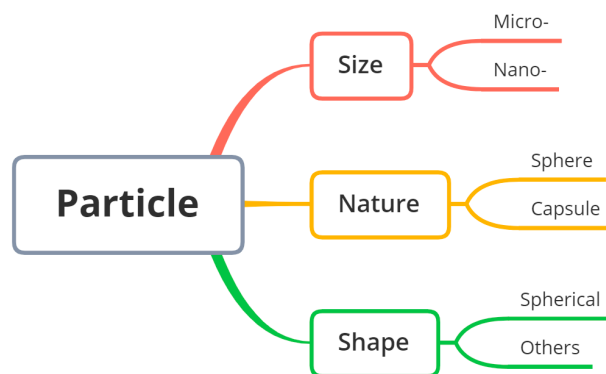


Figure 5. Terminology followed for particulate carriers within the scope of this review.

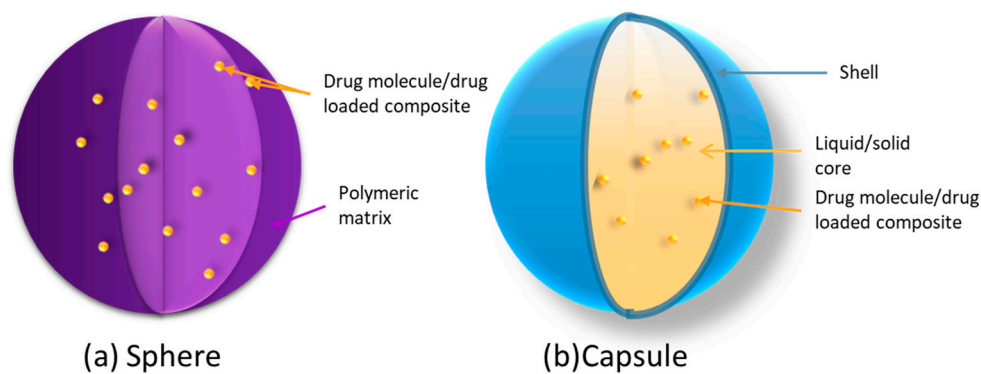


Figure 6. Schematic representation of two types of particulate carriers. (a) Polymeric matrix sphere: drug molecules or drug-loaded composites (micro-/nanoparticles) are dispersed both onto carrier surface and into inner sphere matrix. (b) Solid/liquid core-shell capsule: drug molecules or drug-loaded composites (micro-/nanoparticles, emulsions, liposomes) are entrapped in the liquid/solid core, which is itself enclosed by a shell-like wall.

Table 2. Summary of definitions of nano- and microparticles.

Terminology	Concise Definition
Nanoparticle	Particle of any shape with at least one characteristic dimension between 10^{-9} and 10^{-7} m
Nanocapsule	Hollow nanoparticle consisting of a solid shell encircling a core-forming area
Nanosphere	Spherical-shaped nanoparticle without membrane or any distinct outer layer
Microparticle	Particle with at least one dimension between 10^{-7} and 10^{-4} m
Microcapsule	Hollow microparticle composed of a solid shell surrounding a core-forming space
Microsphere	Microparticle of spherical shape without membrane or any distinct outer layer

A nano-/microsphere is composed of a matrix where substances can be permanently or temporarily embedded, dissolved or covalently bound. Nano-/microcapsules are sub-microscopic colloidal drug carrier systems composed of an oily/aqueous core surrounded by a thin membrane, which is usually, but not necessarily, made of polymer [39].

From a toxicological and pharmaceutical perspective, vesicular capsules possess an advantage over matrix spheres because of their lower polymer content and high loading capacity for both hydrophilic and lipophilic active molecules [41].

2. Preparation Methods for Chitosan-Based Network and Particulate Structure

Over the last few years, many attempts have been made to develop synthetic methods for CS-based particles, such as ionic gelation [44–46], polyelectrolyte complexation [47–49], emulsion solvent diffusion [50,51], emulsion crosslinking [52,53], spray drying [54,55], supercritical fluid drying [56], electrospraying [57], emulsion droplet coalescence [58], reverse micellar/emulsion methods [59,60] and sieving methods [61].

Due to its mild reaction conditions and simple process, the crosslinking gelation method has been extensively studied. The gelation method usually generates the polymer matrix structure, the coating/shell or the core region of core–shell capsules. There are several CS crosslinking gelation mechanisms that offer numerous possibilities for preparing fine-tuned particulate carriers (Figure 7) [62]. Apart from the required experimental conditions, the various gelation methods differ by the nature of the inter-chain crosslinks (ionic, hydrophobic association, covalent, etc.) and, consequently, their stability, reversibility and timescale, among others.

Schematically, spray drying and supercritical processes can produce monolithic matrix (sphere)-structured particles, while capsule structures can be produced via emulsification (emulsion–alkali coacervation/precipitation, emulsion–emulsion coacervation method), electrospraying and microfluidic processes. Table 3 summarizes frequently used methods for the preparation of CS-involved particulate carriers, their main advantages and shortcomings, the size range of the obtained particles and, when available, a rough estimation of the particle concentration at the process outlet.

The structure of a particulate carrier is strongly related to its preparation method. Therefore, selecting the most suitable preparation process is strongly related to the required structural characteristics and, thus, the targeted application. Process parameters, including pH, temperature, concentration of reagents, mass ratio of polymer and crosslinker/surfactants, nature of colloidal stabilizers and agitation speed, have a strong effect on the carrier's structural properties, such as particle average size, particle size distribution, particle shape, porosity, swelling capacity, degradation rate and diffusivity of the drug through the carrier material [63]. Numerous research studies have explored examples of this relationship using the Design of Experiments (DoE) method [64–66].

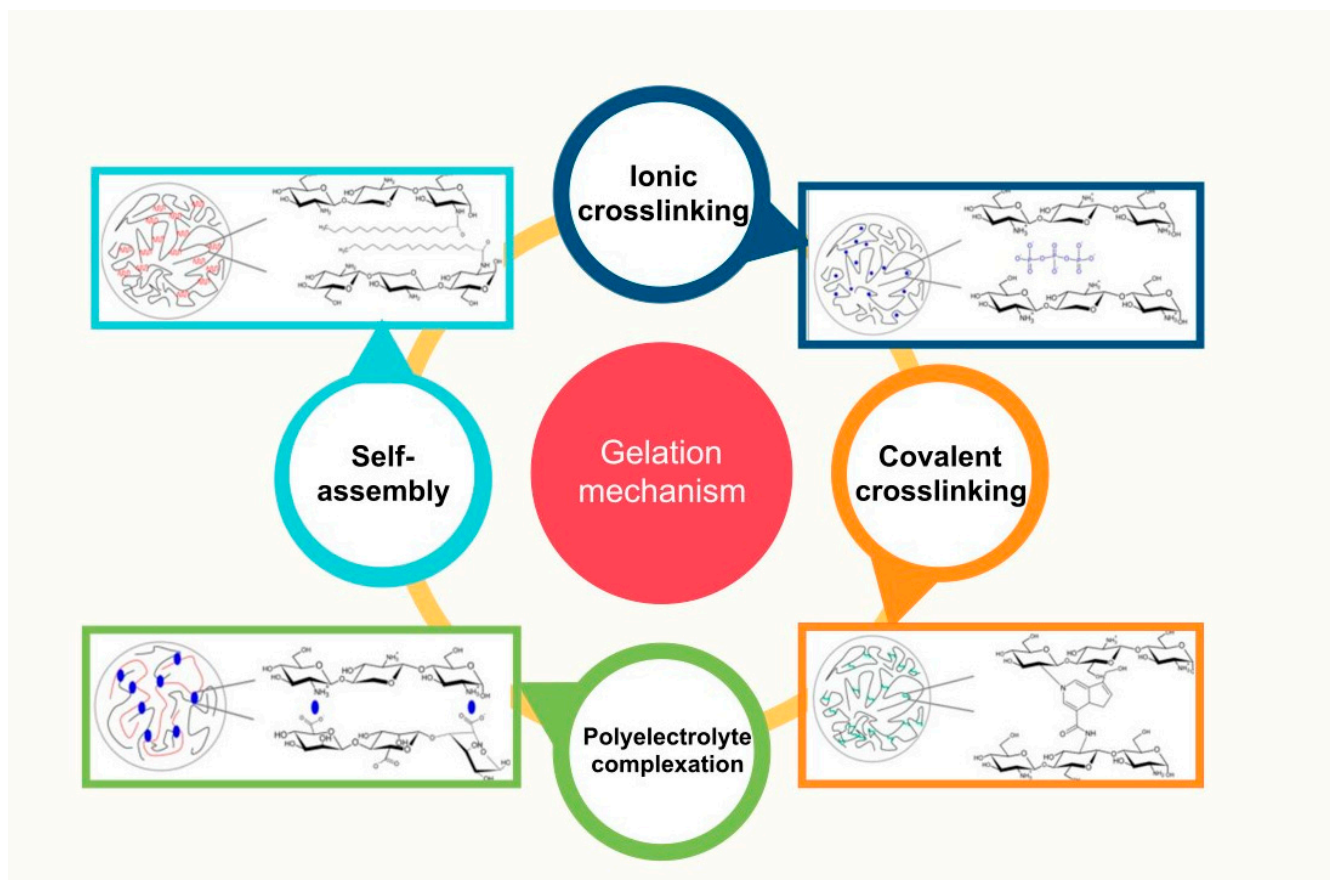


Figure 7. Chitosan crosslinking gelation mechanisms (Adapted from [62] Copyright 2016, Bellich et al.).

For each method reported in the literature, some examples of developed particulate systems were selected and briefly described, along with information about particle size range, morphology of particles (Figure 8), geometrical characteristics of particles and particle concentration.

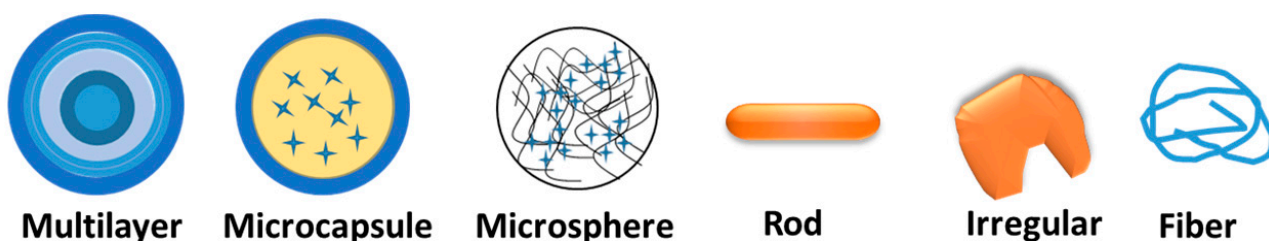


Figure 8. Schematic illustration of chitosan-based particles with various structures.

The parameter “particle concentration” was defined as the concentration of newly-fabricated particles in their dispersing medium after formation but before any extra operations such as separation or dilution. This concentration was calculated or estimated whenever allowed by the provided experimental data. This parameter may be important regarding the scale-up or transfer to industrial processes of lab-scale preparation procedures. Indeed, when very dilute suspensions of particles are produced, further steps may be necessary to increase particle concentration before application.

Table 3. Preparation methods of chitosan relevant particles. Advantages and shortages of each method and geometric dimension of obtained particles. The cartoon symbols present structural characteristics of particles.







Method	Description	Merit (s)	Comments Demerit (s)	Particle Dimension	Geometry of Particle	Particle Concentration (w/v)	Key Parameters	References
Droplet extrusion method	Droplets of drug-loaded polymeric solution are formed by extrusion through a nozzle into a bath of an aqueous solution of polyvalent cations.	The process is convenient, cost-effective and devoid of high temperatures and use of solvent. Also usable for living-cell encapsulation.	Limited size control/size reduction. Difficulties in large-scale production. Teardrop-shaped particles.	90 µm–7 mm		-	Polymer concentration; viscosity of polymer solution; flow rate; geometry of extrusion device; type and concentration of non-solvent bath.	Microcapsule [67]; microsphere [68].
Crosslinking gelation	Electrostatic interaction between polyelectrolytes and polyvalent ions is often used as the driving force to form micro-/nanoparticles. The positively charged natural polymer CS has been broadly investigated to form composites with negative electrolytes by ionic crosslinking (ionotropic gelation). Alternatively, covalent crosslinking has been used.	Mild processing conditions. Simple equipment. Ionotropic gelation: low toxicity, limited risk of altering the encapsulated drug.	Poor stability in non-acidic conditions. Difficulty in encapsulating high-molecular-weight drugs. Toxicity of certain covalent crosslinkers (aldehydes, for instance).	10 nm–3 mm		0.02–1.2%	Polymer concentration; crosslinking agent concentration; mixing rate and time; temperature; pH.	Microsphere [45,46,65,69–82]; microcapsule [83,84].
Polyelectrolyte complexation (PEC)	Complexation of CS with synthetic anionic polyelectrolytes or natural anionic biopolymers via electrostatic interaction.	Able to encapsulate macromolecules such as polypeptides and polynucleotides, as well as hydrophobic drugs.	Toxicity of certain covalent crosslinkers (aldehydes, for instance).	50–450 nm		0.1–2%	Polyelectrolyte concentration; pH; mixing rate and time; temperature; solvent type.	Microsphere [76,84,85]; microcapsule [86].
Complex coacervation/precipitation	CS acetic solution was mixed up with a DNA/protein dissolved salty (sodium sulfate) solution to form micro-/nanospheres.	Narrow particle size distribution; high encapsulation efficiency; relatively low cost of processing.	Safety issue of toxic crosslinkers; poor product formation due to poor solubility of active agent (e.g., plant protein).	50–1600 nm		0.25–0.7%	Nature and concentration of polyelectrolytes; pH; temperature; solvent and co-solvent.	Microsphere [76,87,88].
Emulsion–coacervation (Emulsion–alkali precipitation) method	Drug/oil mixture is dispersed in CS acidic solution under stirring, followed by ultrasonication/homogenization to obtain homogeneous emulsion. Microcapsules were obtained by dropping alkaline solution into aforesaid emulsion.	Devoid of crosslinker.	Suitable for lipophilic drug encapsulation.	10–12 µm		0.05–0.19%	Type and concentration of the polymer, surfactant and alkaline solution; emulsion stirring rate; aging time.	Microcapsule [52,89,90]; double-walled microspheres [78].
Emulsion crosslinking	CS aqueous solution is dispersed into oily phase in the presence of suitable surfactants as emulsion stabilizers. Thermal crosslinking produces microspheres.	Mild processing conditions.	Complete removal of the unreacted crosslinking agent may be difficult due to possible toxicity.	30–700 µm		0.05–1.66%	Polymer concentration; crosslinking agent concentration; mixing speed and time; temperature; pH.	Microspheres [53,91–94]; microsphere-loaded core–shell carrier [50,95].

Table 3. Cont.

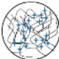
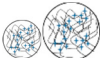
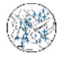





Method	Description	Merit (s)	Comments Demerit (s)	Particle Dimension	Geometry of Particle	Particle Concentration (w/v)	Key Parameters	References
Emulsion solvent diffusion method	An o/w emulsion is prepared by mixing organic solvent into a solution of CS with stabilizer under mechanical stirring, followed by high-pressure homogenization/ultra-sonication. Add a large amount of water to the emulsion to form particles.	High encapsulation efficiency of hydrophobic drugs.	High shear force involved in the process; use of organic solvent.	0.1–45 μm		2%	Solvent selection; emulsification conditions: stirring rate, emulsifying time and temperature.	Micro-/nanosphere [96,97].
Spray-drying method	CS is first dissolved in an aqueous medium, and then the drug is dissolved or dispersed in the previous solution. Crosslinker is added to the polymeric solution. Particles are produced by atomization and subsequent solvent evaporation.	Low impact on the solubility of drug and polymer; simple, reproducible and easy to scale up.	Degradation due to high temperatures or/and high shear rates during atomization.	0.2–60 μm		-	Feed composition and concentration; operation temperature; flow rate and pressure of the atomizing air; spray rate; drying time; type and concentration of the surfactant.	Micro-/nanosphere [54,98–102].
Supercritical technique	Microspheres are fabricated by spraying a drug-loaded HCL/DMSO solution into supercritical carbon dioxide.	Small-sized particles (<3 μm); fast; cost-effective.	Rather broad particle size distribution.	0.4–10 μm		-	Temperature and pressure of the supercritical fluid; solvent type and concentration; flow rate; nozzle geometry; antisolvent addition.	Nanosphere [56]; microsphere [103].
Electrospraying	CS is dispersed/dissolved into a mixture of solvent and blend with drug solution/suspension. The conductive liquids are atomized under high voltage to form drug-encapsulated particles. The flow rate, voltage and distance between needle tip and collector are crucial process parameters.	Low production cost; narrow particle size distribution; easy-to-control surface properties and rapid preparation; high drug-loading efficiency; gentle conditions without use of harsh solvents.	Further investigation needed for upscaling; potential toxicity due to certain solvents.	0.1–1.3 μm		-	Flow rate; solvent evaporation rate; collector distance; electrical conductivity; nature of polymer, solvent and molecules being used in the process.	Nanosphere [57,104,105].
Reverse microemulsion/micellar method	Organic solvent (containing surfactant) is mixed with acidic CS solution to form reverse micelles. Then, drug conjugate and CS attach to the micelles via glutaraldehyde (crosslinker) to form nanoparticles. Residual solvent and surfactant and excess crosslinking agent need to be removed.	Ultrafine particle size (<100 nm); narrow particle size distribution.	Application of organic solvent; time-consuming preparation process; complex washing step.	60–130 nm		0.01–0.1%	Choice of surfactant and co-surfactant; type and concentration of oil phase; water-to-oil ratio; temperature and stirring speed; addition of crosslinking agents.	Nanosphere [59,60,106].
Sieving method	A drug-loaded CS jelly mass is crosslinked and then manually passed through a sieve to obtain non-sticky particles.	Simple and commercially viable; easy scale-up; devoid of tedious processes; high drug loading.	Irregular particle shape.	500–600 μm		-	Mesh size of the sieve; amplitude and frequency of vibration; duration of the sieving process; properties of the material.	Rod- or irregular-shaped microparticles [61].

Table 3. Cont.

Method	Description	Merit (s)	Comments Demerit (s)	Particle Dimension	Geometry of Particle	Particle Concentration (w/v)	Key Parameters	References
Solvent displacement/interfacial deposition method	Sub-microcapsule nanoemulsion coated with CS shell.	Suitable to encapsulate lipophilic drugs; rapid and easy operation; narrow size distribution; absence of shearing stress.	Use of organic solvents.	130–500 nm		0.1–0.33%	Polymer concentration; selection of solvent; selection of non-solvent; mixing rate; temperature; surfactant concentration; pH; addition rate.	Nanocapsule [107–109].
Microfluidic technique	Dispersed phase and continuous phase are syringe-pumped onto microchannel of the microfluidic chip to obtain droplets, which are subsequently hardened by precipitation or crosslinking.	Well-controlled size; able to entrap hydrophilic and/or lipophilic molecules; controllable particles.	Low production rate; difficulties in mass production (scale-up) except parallelization; high cost.	0.2–600 μm		-	Flow rate; viscosity; temperature; device geometry; electrical and magnetic fields.	Microcapsule [47,110,111]; multilayer particle [81,112,113]; microfiber [114].

3. Characteristics of Chitosan-Involved Particulate Carrier

The morphology of sub-microparticles is a fundamental characteristic that significantly affects their properties. Several characteristics of nano-/microparticles are essential to know, such as average size and size distribution, shape, surface properties (area, charge, functionalization), porosity, etc. These properties are desirable for assessing safety, ensuring consistent product quality control and ensuring regulatory compliance.

The size distribution of spherical particles is a subject that has been well illustrated and developed. Briefly, it is generally required to combine light-scattering techniques (DLS, LS) with microscopic characterization using TEM, SEM and AFM [115–118]. However, for non-spherical particles, the diffusion coefficient also depends on the shape of the particles [119,120]. A combination of several techniques is recommended to obtain precise information on particle size and shape. For example, particles with irregular shapes obtained from the sieving method have been characterized by the laser light diffusion method and SEM micrographs. LS was used to determine the size and distribution of spherical particles equal in volume to the samples [61]. As for rod-shaped and cylindrical particles, the aspect ratio was introduced to describe the elongation of the particle shape [119]. The characterization of fiber-shaped particles requires more complex techniques as they have an elongated shape and cannot be adequately described by a single dimension. Size characterization of fiber-shaped particles can be conducted based on various dimensions such as diameter, length, aspect ratio and specific surface area [120–123]. Finally, it must be reminded that average values of particle size may differ from one technique to another simply because “averages” are not calculated in the same way (number, surface, volume, intensity, etc.).

Additionally, Small-angle X-ray scattering (SAXS) is a technique that can be used to determine the size, size distribution, shape and organization of hierarchical structures [124]. SAXS is based on the interaction of X-rays with the electrons in the material, producing scattering patterns that can interpret particle shapes such as spheres, rods, discs, hollow spheres and dumbbells [125]. However, SAXS is limited to analyzing samples in the range of 1–100 nanometers, and interpreting SAXS data, especially when the sample is complex or contains multiple components, could be challenging.

As to capsule and multilayer particles, besides the size of the particle (the diameter of the outermost shell), the thickness of the layer(s) (including shell thickness) is also an interesting characteristic to know since the properties of layers made of different materials can be pretty diverse. However, this characteristic has not been abundantly discussed in the literature.

Microscopy techniques (SEM, TEM, CLSM) play a significant role not only by visualizing the surface morphology, shape and size of sub-microparticles but also their internal structure (cross-section, porosity, crystallinity) [113,126–129]. Additionally, the structural evolution of particles during the release process can be monitored by consecutive micrographs, which can reveal and confirm the release mechanism over time [130]. SEM and TEM can provide high-resolution images of the particle structure and morphology, allowing for direct visualization of the particles at the nanoscale. Confocal microscopy uses a focused laser beam to scan a sample and create a series of optical sections at different depths. Confocal slices can provide detailed information about the internal structure and organization of the sample at a particular depth or plane (Figure 9). By using fluorescent labeling, the oil phase inside the core of microcapsules was localized and quantified [130]. The fluorescence signals of polymers allow the visualization of their distribution within the polymeric shell. Furthermore, the oil phase is distinguished unambiguously from air bubbles by comparing optical and fluorescent images. With the help of computational image analysis, the layer thickness and the volumes of different phases can be estimated.

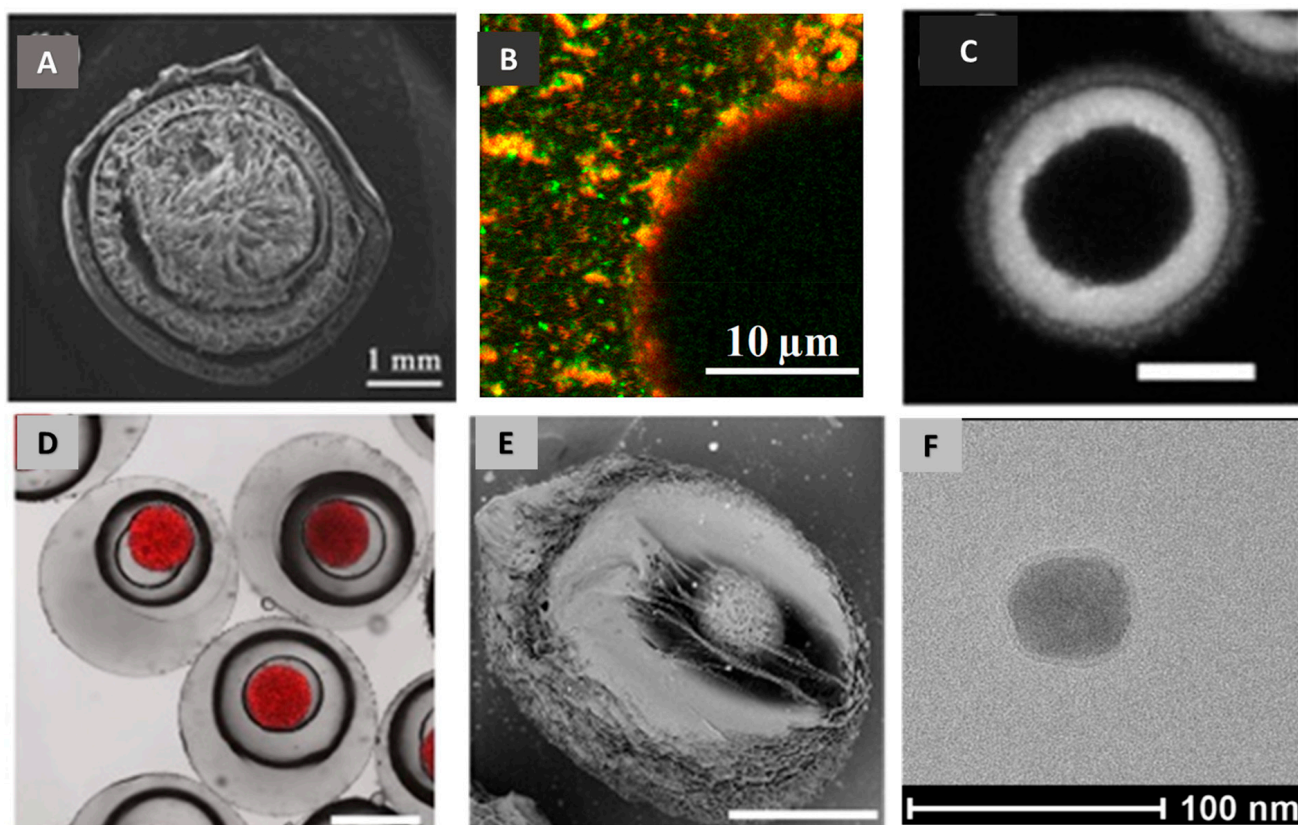


Figure 9. Internal structure and layer thickness of particles can be characterized by SEM, CLSM and TEM images. (A) Cross-sectional morphologies (SEM) of three-layer CS hydrogel capsules (adapted with permission from Ref. [81]. Copyright 2019, Elsevier); (B) CLSM picture of fresh oil-in-water CS emulsion (adapted with permission from Ref. [131]. Copyright 2020, Elsevier); (C) CLSM fluorescence image of CS-coated microcapsule, scale bar = 5 μm (adapted with permission from Ref. [132]. Copyright 2012, Wiley); (D) CLSM image of O1/W2/O3/W4/O5 microcarriers; (E) SEM image of dual-responsive microcarriers without O1 and O3 cores. Scale bars are 200 μm , adapted with permission from Ref. [112]. Copyright 2019, Elsevier; (F) TEM image of CS nanoparticle with particle size of around 45 nm and silica shell thickness of 5 nm (adapted from Ref. [133]. Copyright 2019, Arzumanyan G, et al.).

4. Particulate Structure and Controlled Release Kinetics

Drug release refers to the process by which entrapped drugs dissolve and diffuse into the outer medium by diffusing within bulk core material and/or shell material or passing through pores or fractures within the particles. Drug release kinetics depend greatly on the particulate building materials, drug properties and structural properties of composites, including shape, particle size, surface roughness, porosity, shell thickness, etc. Additionally, along the release process, carrier structure may evolve under the effect of stimuli in the release environment. The assumed principal drug release mechanisms include dissolution, erosion, swelling and diffusion [20,134]. Release mechanisms and the corresponding release profiles dominated by each were summarized in Ref. [62]. To simplify the analysis of the experimental release results, it is generally crucial to identify the limiting phenomena.

As the drug release process results from interactions between entrapped molecules, encapsulating particles and the releasing environment, the particulate structure and its evolution over a definite release time have a great effect on release kinetics. Elucidating the corresponding relations between composite structures and potential release mechanisms enables researchers to predict the release trend of certain loaded active ingredients from a specific structured vehicle. Figure 10 summarizes graphically several typical CS-involved

particulate carriers with relevant release profiles found in the literature. In Figure 10a, which illustrates CS polymeric matrix particles, drug molecules are distributed on the particle surface as well as inside the matrix. The diffusion of molecules located superficially may lead to a burst release, i.e., the fast release of a significant number of loaded molecules before the further and slower release of the remaining substance. Medium permeation inward the carrier causes erosion, swelling and diffusion, which are mainly responsible for the following sustained release, which may last from hours to days [83,111]. Figure 10b represents a core-shell capsule case. The core region could be solid or liquid (oil phase), which encapsulates dissolved active ingredients or dispersed systems such as emulsion droplets, nano-/microparticles or liposomes [82,112,135]. The outer wall-like shell prevents leakage and the degradation of the inner contents from harsh conditions inside the internal environment, such as pH, enzymes, etc. Structural incompleteness due to fracture or breakage of the shell leads to the liberation of inside molecules. Figure 10c is a core-shell-structured microcapsule encapsulating drug-loaded nanoparticles in an oily core enclosed by a CS shell. Both drug molecules and drug-loaded poly-(lactic-co-glycolic acid) (PLGA) nanoparticles were enclosed in a stimulus-responsive microcapsule [110]. The CS shell prevented the leakage of the entrapped cargo in a neutral medium and broke down in an acidic site, thus providing sustained drug delivery through the diffusion of free drug and nanoparticle degradation. Additionally, enzyme intestinal delivery was reported to be localized by alginate nanoparticles incorporated into CS-shelled microcapsules [113]. Figure 10d is a CS-based microsphere with an alginate coating. The coating can protect the loaded substance from degradation and hydrolysis in acidic conditions for hours and can modulate the release rate by suppressing burst release [103]. In addition, in some other core-shell cases, the external shell is able to respond to certain stimuli, e.g., pH and ionic strength [82], and achieve targeting effects through the addition of biological ligands [84]. Figure 10e,f are both multilayered CS hydrogel capsules. The drug is loaded homogeneously in each layer of the carrier in Figure 10e, while the one in Figure 10f contains sequentially alternating drug-loaded and void layers. It is possible to customize the number of layers and tailor their thickness [136]. The former achieves approximately a zero-order release, while the latter is supposed to attain a pulsatile drug release [81]. Apart from CS-based carriers alone, the encapsulated ingredient is also a dimension that can enrich the utility of these functional carriers. For example, Figure 10g represents a core-shell nanosphere system that was developed for co-delivering drugs (oleanolic acid and doxorubicin) as a strategy to treat multi-drug-resistant breast cancer. This novel dual-drug-loaded DDS was proven effective as a breast-tumor targeting strategy in *in vitro* and *ex vivo* evaluations [137]. Below are some typical CS-relevant carriers with their release profiles found in the literature. Particularly worth mentioning is the fact that certain release profiles may be attained by diverse carriers. Inversely, a carrier may possess different release profiles under different dissolution conditions (pH, ionic strength, light, temperature, magnetic field, etc.).

To sum up, further investigations into the correlation between carrier structure and the associated release profile are worth the effort. By achieving this goal, in turn, it would be possible to design on-demand drug delivery systems that can regulate, in an expected way, more precisely the release rate of certain drugs at a specific time interval and location.

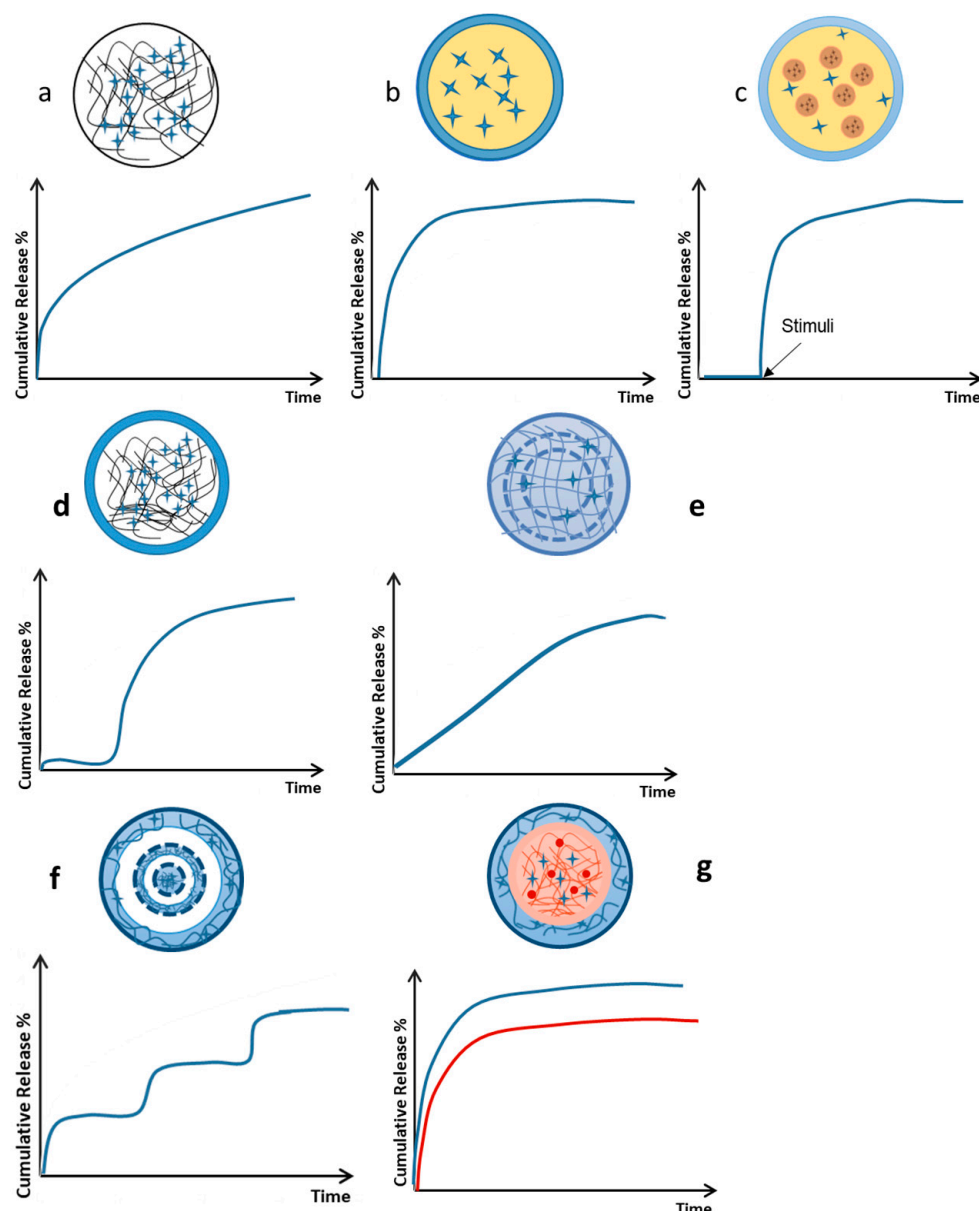


Figure 10. Schematic illustration of typical chitosan sub-microparticulate carriers and corresponding release profiles found in the literature. The shuriken-shaped blue marks and red dots stand for active ingredients loaded. (a) Monolithic sphere; (b) capsule with liquid core; (c) nanoparticle-loaded capsule with CS shell; (d) core-shell sphere with CS matrix core; (e,f) multilayered CS hydrogel capsule; (g) core-shell sphere loading two drugs.

5. Release Kinetics, Mechanisms and Modeling

The use of kinetic models can aid in describing the release rate of drugs, leading to increased efficiency, accuracy and safety of the dose. This, in turn, can help optimize the design of drug delivery devices [138]. With an appropriate understanding of the limiting phenomena that govern drug release from a given system, it is possible to describe drug release behavior by applying proper mathematical models. As known, various factors greatly influence this complex process, such as matrix geometry, matrix swelling equilibrium and kinetics, matrix erosion, drug dissolution and partitioning, drug diffusion, drug-matrix interaction, initial drug distribution, etc. (Figure 11). Based on specific assumptions and hypotheses, certain mathematical models enable the simulation of release kinetics under certain conditions. Some of these mathematical models have been commonly

used to identify dominant release mechanisms on the basis of the comparison between experimental and theoretical time variations in cumulated released amounts [138].

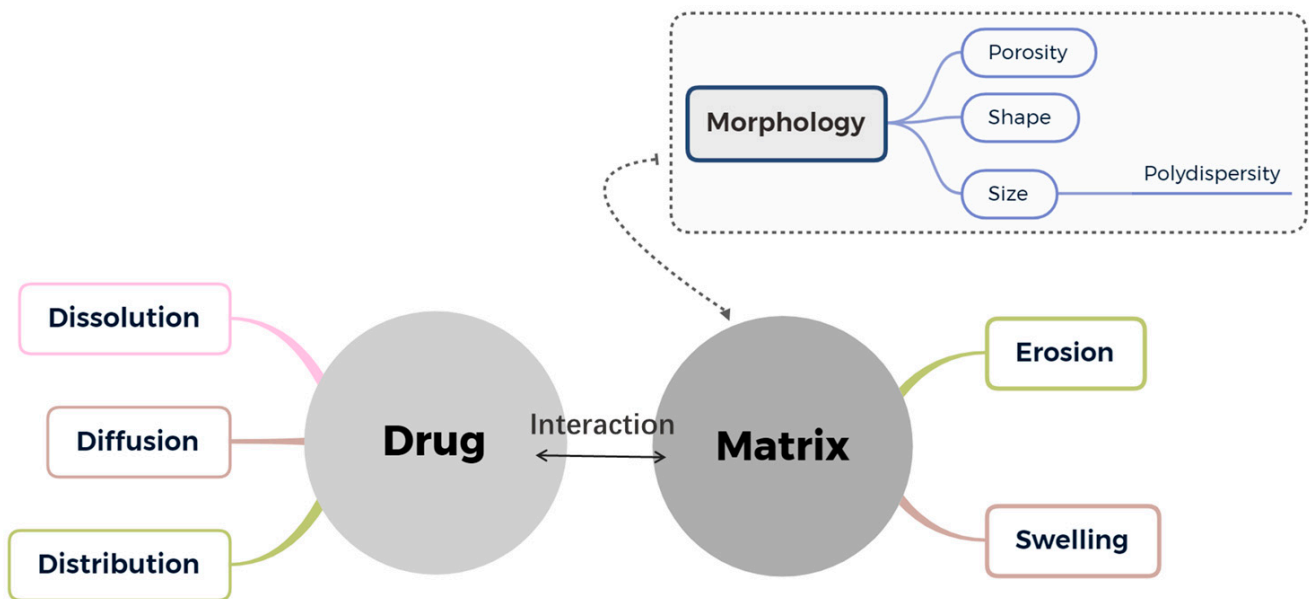


Figure 11. Factors influencing drug release kinetics.

Trying to develop a general and unifying model would consequently result in an increase in the complexity of the model's expression and make it difficult to obtain analytical and/or numerical solutions. Although achieving a highly general model may be challenging, researchers have explored the potential of using empirical/semi-empirical models to describe the release kinetic characteristics, prioritizing various aspects that make up the release phenomenon. Mathematical models used to fit the drug release profile from CS-based particles include the Higuchi square root, Korsmeyer–Peppas', Hixon–Crowell's, Baker–Lonsdale's, Peppas–Sahlin's, Kopcha's, Hopfenberg's and Gallagher–Corrigan (GC) models. According to the systems, zero-order or first-order kinetics may be observed.

For zero-order kinetics, the release of an active agent is only a function of time, and the process takes place at a constant rate independent of active agent concentration:

$$M_t = kt \quad (1)$$

where M_t is the amount of drug released at time t and k is the zero-order constant.

The first-order release kinetics model assumes that the rate of drug release is proportional to the amount of drug remaining in the dosage form [139,140]:

$$1 - \frac{M_t}{M_0} = e^{-k't}$$

where k' is the first-order rate constant and M_0 is the initial amount of drug in the dosage form.

The Higuchi model explains the release of a drug as a diffusion process, which is governed by Fick's law and has a time-dependent square root relationship [141]:

$$\frac{M_t}{M_\infty} = k_H \sqrt{t} \quad (2)$$

where M_∞ is the absolute amount of drug released over infinite time and k_H is a release rate constant.

The Korsmeyer–Peppas model is a semi-empirical model that establishes the exponential relationship between the amount released and the time and provides indications about the mechanism of drug release [142–144]:

$$\frac{M_t}{M_\infty} = Kt^n \quad (3)$$

where K is a rate constant and n is the exponent that incorporates the effects of the release mechanism and the geometrical characteristics of the system.

The Hixson–Crowell model was initially derived from a work dealing with agitation [145]:

$$\sqrt[3]{M_0} = \sqrt[3]{M_0 - M_t} + K_{HC}t \quad (4)$$

where K_{HC} is the constant of incorporation, which relates surface and volume.

The Peppas–Sahlin model assumes that drug release occurs through diffusion with a simultaneous influence of polymer relaxation and that it is possible to include the two contributions by summation (diffusional and relaxational terms) [146]:

$$\frac{M_t}{M_\infty} = k_d t^m + k_r t^{2m} \quad (5)$$

where k_d and k_r are the kinetic constants of diffusion and relaxation, respectively, and m is the diffusion exponent.

Kopcha's model [147], also relying on the assumption of summation, includes simultaneous diffusion and erosion contributions within the release kinetics:

$$M_t = Bt + A\sqrt{t} \quad (6)$$

where A and B are the diffusion constant and erosion constant, respectively.

Based on the Higuchi model, the Baker–Lonsdale model was developed for controlled drug release from spherical matrices [148]:

$$\frac{3}{2} \left[1 - \left(1 - \frac{M_t}{M_\infty} \right)^{\frac{2}{3}} \right] - \frac{M_t}{M_\infty} = k'' t \quad (7)$$

where k'' is the release constant, which corresponds to the slope of the experimental curve [149,150]. This equation can be utilized for the linearization of release data for many microparticle formulations [143].

Hopfenberg derived a model to explain the release of drugs from an erodible system in the case of a spherical particle [151]:

$$\frac{M_t}{M_\infty} = 1 - \left[1 - \frac{k_0 t}{C_0 a_0} \right]^3 \quad (8)$$

where k_0 is the erosion rate constant, C_0 is the initial concentration of drug in the matrix and a_0 is the initial radius.

The Gallagher–Corrigan (GC) model was applied to evaluate drug release from biodegradable polymeric drug delivery systems by combining diffusion and polymer relaxation/degradation contributions:

$$\frac{M_t}{M_\infty} = A_1(1 - e^{-k_1 t}) + A_2 \frac{e^{k_2(t-t_m)}}{1 + e^{k_2(t-t_m)}} \quad (9)$$

where A_1 and A_2 are constants related to the contributions of the diffusion and relaxation mechanisms to drug release, k_1 is the release constant in the first stage, t_m is the maximum release time and k_2 is the release constant during the stage of polymer degradation.

The GC model is particularly useful for predicting drug release profiles under different conditions [152]. Additionally, it can be adapted to describe dual-phased drug release [152–154]. The experimental data on the release of curcumin from MnFe₂O₄ magnetic nanoparticles with multilayered CS–alginate (ALG) shells were a good fit to the GC model. The CS–ALG coating was reported to be useful in inhibiting burst release, and the increase in the number of layers could delay the dissolution rate, thus achieving sustained release [154].

The distinguishing aspect of the last three models from others is their incorporation of two discrete phenomena that occur during drug release: diffusion and relaxation in the Peppas–Sahlin and Gallagher–Corrigan models and diffusion and erosion in Kopcha’s model.

Frequently used models are adopted to describe the release characteristics and mechanisms of drugs from CS-based systems, prioritizing different factors (Table 4).

Table 4. Mathematical models to reveal the release mechanisms of reported chitosan-based particulate systems.

Mechanism (s)	Description of Systems	Model	Equation(s)	References
Diffusion	Crosslinked CS-dextran sulfate nanoparticle	Higuchi	(2)	[85]
	Crosslinked CS microspheres	Korsmeyer–Peppas/Higuchi	(3)(2)	[94]
	Spray-Dried CS Microspheres	Higuchi/Korsmeyer	(2)(3)	[155]
	CS hydrogel	Zero-order kinetic	(1)	
	Fatty acid-grafted CS hydrogel	Higuchi	(2)	[156]
	CS-LLA ⁱ	Hixson	(4)	
Diffusion and relaxation	CS–alginate nanoparticles	Korsmeyer–Peppas	(3)	[157]
	CS–genipin matrices	Peppas–Sahlin	(5)	[158]
	Multilayer CS–alginate-coated nanocarrier	Gallagher–Corrigan	(9)	[154]
	Alginate–carboxymethylcellulose microparticles with CS shells	Gallagher–Corrigan	(9)	[152]
Diffusion and swelling	CS–alginate	Hopfenberg	(8)	[159]
Diffusion, erosion	DOX-loaded PLGA-QCS ⁱⁱ core–shell polymersomes	Korsmeyer–Peppas	(3)	[160]
		Kopcha	(6)	
	PLGA/CS microcapsules	Baker–Lonsdale	(7)	[161]

ⁱ LLA: linolenic acid; ⁱⁱ QCS: Chitosan Quaternary Ammonium Salt.

It is important to note that good-fitting experimental data are necessary but may not be sufficient to identify the best model among different models devoted to correctly describing complex release kinetics. Mathematical hypotheses are supposed to take experimental observation of phenomena into consideration. However, in practice, it may not always be feasible. For instance, swelling and erosion of the CS matrix also contributed to the release of vitamins, but the best model chosen was the Peppas–Sahlin model, which privileges more diffusion and relaxation [158]. By synthetically analyzing characteristic constants of diverse models, researchers can better understand the underlying mechanisms of drug release and predict the release kinetics more accurately [1].

Furthermore, considering the overall size distribution of particles rather than just the unitary average diameter may be crucial in developing more accurate models, as heterogeneity in samples is a common occurrence in practical applications [162,163].

It is noteworthy that the systematic implementation of mathematical modeling in the development of active ingredient delivery systems can enhance R&D efficiency, save time and reduce expenses. Additionally, the advanced utilization of this approach can enable the advancement of precision medicine. Instead of an undifferentiated regular dosage

regimen, personalized medicine can afford a better therapeutic effect and lower toxicity by considering patients' individual characteristics.

6. Conclusive Remarks and Prospective Research

Tremendous interest in CS from both academic and diverse industrial fields has emerged over the past few decades. Innovative carriers have been developed with unique properties such as sustained release, responsiveness to environmental factors and multi-phase release.

An improved understanding of the close relationship between the preparation process and particle structure would enable the prediction of formulation and preparation strategies for drug delivery systems to achieve the desired release kinetics [152,164]. Additionally, modeling capacity is a powerful tool to increase the efficiency of developing new systems, which is crucial for the industry to turn the idea of on-demand drug delivery systems (DDS) into a reality.

Efforts should be focused on investigating in a more specific manner how the preparation process affects the structure of the vehicle and subsequent release behaviors from the polymeric network. By gaining more insight into these aspects, it is possible to design DDSs that release drugs in a controlled manner, such as sustained release, pulsatile release or targeted release, depending on the specific therapeutic needs.

Author Contributions: Conceptualization and methodology, A.D., S.D.; writing—original draft preparation, J.W.; writing—review and editing, A.D., S.D., J.W.; supervision, A.D., S.D.; funding acquisition, S.D. All authors have read and agreed to the published version of the manuscript.

Funding: This is work supported by the “Impact Biomolecules” project of the “Lorraine Université d’Excellence” (Investissements d’avenir–ANR project number 15-004).

Institutional Review Board Statement: Not applicable.

Informed Consent Statement: Not applicable.

Data Availability Statement: Not applicable.

Acknowledgments: The authors gratefully acknowledge the financial support from the “Impact Biomolecules” project of the “Lorraine Université d’Excellence”.

Conflicts of Interest: The authors declare no conflict of interest.

References

1. Tharanathan, R.N.; Kittur, F.S. Chitin—The Undisputed Biomolecule of Great Potential. *Crit. Rev. Food Sci. Nutr.* **2003**, *43*, 61–87. [[CrossRef](#)] [[PubMed](#)]
2. Zeng, J.-B.; He, Y.-S.; Li, S.-L.; Wang, Y.-Z. Chitin Whiskers: An Overview. *Biomacromolecules* **2012**, *13*, 1–11. [[CrossRef](#)] [[PubMed](#)]
3. Shit, S.C.; Shah, P.M. Edible Polymers: Challenges and Opportunities. *J. Polym.* **2014**, *2014*, 1–13. [[CrossRef](#)]
4. Martínez, J.P.; Falomir, M.P.; Gozalbo, D. Chitin: A Structural Biopolysaccharide with Multiple Applications. In *eLS*; American Cancer Society: Atlanta, GA, USA, 2014; ISBN 978-0-470-01590-2.
5. Abd El-Hack, M.E.; El-Saadony, M.T.; Shafi, M.E.; Zabermaawi, N.M.; Arif, M.; Batiha, G.E.; Khafaga, A.F.; Abd El-Hakim, Y.M.; Al-Sagheer, A.A. Antimicrobial and Antioxidant Properties of Chitosan and Its Derivatives and Their Applications: A Review. *Int. J. Biol. Macromol.* **2020**, *164*, 2726–2744. [[CrossRef](#)]
6. Gooday, G.W. The Ecology of Chitin Degradation. In *Advances in Microbial Ecology*; Marshall, K.C., Ed.; Springer: Boston, MA, USA, 1990; pp. 387–430.
7. Latańska, I.; Rosiak, P.; Paul, P.; Sujka, W.; Kolesińska, B.; Latańska, I.; Rosiak, P.; Paul, P.; Sujka, W.; Kolesińska, B. *Modulating the Physicochemical Properties of Chitin and Chitosan as a Method of Obtaining New Biological Properties of Biodegradable Materials*; IntechOpen: London, UK, 2021; ISBN 978-1-78984-425-2.
8. Kim, S.-K. *Chitin, Chitosan, Oligosaccharides and Their Derivatives: Biological Activities and Applications*, 1st ed.; CRC Press: Boca Raton, FL, USA, 2010; ISBN 978-1-4398-1603-5.
9. Shariatinia, Z. Pharmaceutical Applications of Chitosan. *Adv. Colloid Interface Sci.* **2019**, *263*, 131–194. [[CrossRef](#)]
10. Aranaz, I.; Alcántara, A.R.; Civera, M.C.; Arias, C.; Elorza, B.; Heras Caballero, A.; Acosta, N. Chitosan: An Overview of Its Properties and Applications. *Polymers* **2021**, *13*, 3256. [[CrossRef](#)]
11. Zhou, D.-Y.; Wu, Z.-X.; Yin, F.-W.; Song, S.; Li, A.; Zhu, B.-W.; Yu, L.-L. (Lucy). Chitosan and Derivatives: Bioactivities and Application in Foods. *Annu. Rev. Food Sci. Technol.* **2021**, *12*, 407–432. [[CrossRef](#)]

12. Food and Agriculture Organization of United Nations. *The State of World Fisheries and Aquaculture 2014.*; FAO: Rome, Italy, 2014.
13. Yan, N.; Chen, X. Sustainability: Don't Waste Seafood Waste. *Nat. News* **2015**, *524*, 155. [[CrossRef](#)]
14. EUCHIS European Chitin Society-Euchis.Org. Available online: <https://euchis.org/> (accessed on 22 February 2023).
15. Riofrio, A.; Alcivar, T.; Baykara, H. Environmental and Economic Viability of Chitosan Production in Guayas-Ecuador: A Robust Investment and Life Cycle Analysis. *ACS Omega* **2021**, *6*, 23038–23051. [[CrossRef](#)]
16. Alibaba Chitosan Price, 2023 Chitosan Price Manufacturers & Suppliers | Made-in-China.com. Available online: https://www.made-in-china.com/multi-search/Chitosan_Price/F2--CL_DM--PV_1356080000_19114_4374/1.html (accessed on 6 March 2023).
17. SFLY. PRODUCTEUR DE CHITINE, CHITOSAN-HERMETIA ILLUCENS. *SFLY*. Available online: <http://sflyproteins.fr/> (accessed on 29 March 2019).
18. Factors, F. Chitosan Industry Trends, Share, Value, Analysis & Forecast Report. 2022. Available online: <https://www.globenewswire.com/en/news-release/2022/09/27/2523512/0/en/Demand-for-Global-Chitosan-Market-Size-to-Hit-26272-32-Mn-by-2028-Exhibit-a-CAGR-of-24-10-Chitosan-Industry-Trends-Share-Value-Analysis-Forecast-Report-by-Facts-Factors.html> (accessed on 28 February 2023).
19. Report Linker. Global Chitin and Chitosan Derivatives Market to Reach \$24.9 Billion by 2030. Available online: <https://www.globenewswire.com/news-release/2023/02/17/2610744/0/en/Global-Chitin-and-Chitosan-Derivatives-Market-to-Reach-24-9-Billion-by-2030.html> (accessed on 6 March 2023).
20. Munawar, A.M.; Syeda, J.; Wasan, K.; Wasan, E. An Overview of Chitosan Nanoparticles and Its Application in Non-Parenteral Drug Delivery. *Pharmaceutics* **2017**, *9*, 53. [[CrossRef](#)]
21. Jing, H.; Guo, Z.; Guo, W.; Yang, W.; Xu, P.; Zhang, X. Synthesis and Characterization of Folic Acid Modified Water-Soluble Chitosan Derivatives for Folate-Receptor-Mediated Targeting. *Bioorg. Med. Chem. Lett.* **2012**, *22*, 3418–3424. [[CrossRef](#)]
22. Azmana, M.; Mahmood, S.; Hilles, A.R.; Rahman, A.; Arifin, M.A.B.; Ahmed, S. A Review on Chitosan and Chitosan-Based Bionanocomposites: Promising Material for Combatting Global Issues and Its Applications. *Int. J. Biol. Macromol.* **2021**, *185*, 832–848. [[CrossRef](#)]
23. Masuko, T.; Minami, A.; Iwasaki, N.; Majima, T.; Nishimura, S.I.; Lee, Y.C. Thiolation of Chitosan. Attachment of Proteins via Thioether Formation. *Biomacromolecules* **2005**, *6*, 880–884. [[CrossRef](#)]
24. Knight, D.K.; Shapka, S.N.; Amsden, B.G. Structure, Depolymerization, and Cytocompatibility Evaluation of Glycol Chitosan. *J. Biomed. Mater. Res. Part A* **2007**, *83A*, 787–798. [[CrossRef](#)]
25. Kim, K.; Kim, J.H.; Kim, S.; Chung, H.; Choi, K.; Kwon, I.C.; Park, J.H.; Kim, Y.S.; Park, R.W.; Kim, I.S.; et al. Self-Assembled Nanoparticles of Bile Acid-Modified Glycol Chitosans and Their Applications for Cancer Therapy. *Macromol. Res.* **2005**, *13*, 167–175. [[CrossRef](#)]
26. Zheng, Y.; Cai, Z.; Song, X.; Yu, B.; Bi, Y.; Chen, Q.; Zhao, D.; Xu, J.; Hou, S. Receptor Mediated Gene Delivery by Folate Conjugated N-Trimethyl Chitosan in Vitro. *Int. J. Pharm.* **2009**, *382*, 262–269. [[CrossRef](#)]
27. Wang, F.; Zhang, D.; Duan, C.; Jia, L.; Feng, F.; Liu, Y.; Wang, Y.; Hao, L.; Zhang, Q. Preparation and Characterizations of a Novel Deoxycholic Acid-O-Carboxymethylated Chitosan-Folic Acid Conjugates and Self-Aggregates. *Carbohydr. Polym.* **2011**, *84*, 1192–1200. [[CrossRef](#)]
28. Li, D.-H.; Liu, L.-M.; Tian, K.-L.; Liu, J.-C.; Fan, X.-Q. Synthesis, Biodegradability and Cytotoxicity of Water-Soluble Isobutylchitosan. *Carbohydr. Polym.* **2007**, *67*, 40–45. [[CrossRef](#)]
29. Engibaryan, L.G.; Chernukhina, A.I.; Gabrielyan, G.A.; Gal'braikh, L.S. Fabrication of New Water-Soluble Chitosan Derivatives. *Fibre Chem.* **2005**, *37*, 285–288. [[CrossRef](#)]
30. Liu, S.-H.; Chen, R.-Y.; Chiang, M.-T. Effects and Mechanisms of Chitosan and Chitosan Oligosaccharide on Hepatic Lipogenesis and Lipid Peroxidation, Adipose Lipolysis, and Intestinal Lipid Absorption in Rats with High-Fat Diet-Induced Obesity. *Int. J. Mol. Sci.* **2021**, *22*, 1139. [[CrossRef](#)]
31. Ait Hamdan, Y.; El Amerany, F.; Desbrières, J.; Aghrinane, A.; Oudadesse, H.; Rhazi, M. The Evolution of the Global COVID-19 Epidemic in Morocco and Understanding the Different Therapeutic Approaches of Chitosan in the Control of the Pandemic. *Polym. Bull.* **2022**, 1–27. [[CrossRef](#)] [[PubMed](#)]
32. Hanafy, N.A.N.; El-Kemary, M.A. Silymarin/Curcumin Loaded Albumin Nanoparticles Coated by Chitosan as Muco-Inhalable Delivery System Observing Anti-Inflammatory and Anti COVID-19 Characterizations in Oleic Acid Triggered Lung Injury and in Vitro COVID-19 Experiment. *Int. J. Biol. Macromol.* **2022**, *198*, 101–110. [[CrossRef](#)]
33. Landauer, J.; Kuhn, M.; Nasato, D.S.; Foerst, P.; Briesen, H. Particle Shape Matters-Using 3D Printed Particles to Investigate Fundamental Particle and Packing Properties. *Powder Technol.* **2020**, *361*, 711–718. [[CrossRef](#)]
34. Dasgupta, S.; Auth, T.; Gompper, G. Shape and Orientation Matter for the Cellular Uptake of Nonspherical Particles. *Nano Lett.* **2014**, *14*, 687–693. [[CrossRef](#)] [[PubMed](#)]
35. Ching, S.H.; Bansal, N.; Bhandari, B. Alginate Gel Particles-A Review of Production Techniques and Physical Properties. *Crit. Rev. Food Sci. Nutr.* **2017**, *57*, 1133–1152. [[CrossRef](#)] [[PubMed](#)]
36. Saleem, S.; Animasau, I.L.; Yook, S.-J.; Al-Mdallal, Q.M.; Shah, N.A.; Faisal, M. Insight into the Motion of Water Conveying Three Kinds of Nanoparticles Shapes on a Horizontal Surface: Significance of Thermo-Migration and Brownian Motion. *Surf. Interfaces* **2022**, *30*, 101854. [[CrossRef](#)]

37. Chen, M.-M.; Cao, H.; Liu, Y.-Y.; Liu, Y.; Song, F.-F.; Chen, J.-D.; Zhang, Q.-Q.; Yang, W.-Z. Sequential Delivery of Chlorhexidine Acetate and BFGF from PLGA-Glycol Chitosan Core-Shell Microspheres. *Colloids Surf. B Biointerfaces* **2017**, *151*, 189–195. [[CrossRef](#)]
38. Tsai, M.-S.; Li, M.J. A Novel Process to Prepare a Hollow Silica Sphere via Chitosan-Polyacrylic Acid (CS-PAA) Template. *J. Non-Cryst. Solids* **2006**, *352*, 2829–2833. [[CrossRef](#)]
39. Vert, M.; Doi, Y.; Hellwich, K.-H.; Hess, M.; Hodge, P.; Kubisa, P.; Rinaudo, M.; Schué, F. Terminology for Biorelated Polymers and Applications (IUPAC Recommendations 2012). *Pure Appl. Chem.* **2012**, *84*, 34. [[CrossRef](#)]
40. Guterres, S.S.; Alves, M.P.; Pohlmann, A.R. Polymeric Nanoparticles, Nanospheres and Nanocapsules, for Cutaneous Applications. *Drug Target Insights* **2007**, *2*, 117739280700200. [[CrossRef](#)]
41. Couvreur, P.; Barratt, G.; Fattal, E.; Vauthier, C. Nanocapsule Technology: A Review. *Crit. Rev. Ther. Drug Carr. Syst.* **2002**, *19*. [[CrossRef](#)]
42. Schaffazick, S.R.; Guterres, S.S.; Freitas, L.D.L.; Pohlmann, A.R. Physicochemical Characterization and Stability of the Polymeric Nanoparticle Systems for Drug Administration. *Quím. Nova* **2003**, *26*, 726–737. [[CrossRef](#)]
43. Mehnert, W.; Mäder, K. Solid Lipid Nanoparticles: Production, Characterization and Applications. *Adv. Drug Deliv. Rev.* **2012**, *64*, 83–101. [[CrossRef](#)]
44. Lin, Y.-H.; Chang, C.-H.; Wu, Y.-S.; Hsu, Y.-M.; Chiou, S.-F.; Chen, Y.-J. Development of PH-Responsive Chitosan/Heparin Nanoparticles for Stomach-Specific Anti-Helicobacter Pylori Therapy. *Biomaterials* **2009**, *30*, 3332–3342. [[CrossRef](#)]
45. Arozal, W.; Louisa, M.; Rahmat, D.; Chendrana, P.; Sandhiutami, N.M.D. Development, Characterization and Pharmacokinetic Profile of Chitosan-Sodium Tripolyphosphate Nanoparticles Based Drug Delivery Systems for Curcumin. *Adv. Pharm. Bull.* **2021**, *11*, 77–85. [[CrossRef](#)]
46. Gooneh-Farahani, S.; Naghib, S.M.; Naimi-Jamal, M.R. A Novel and Inexpensive Method Based on Modified Ionic Gelation for PH-Responsive Controlled Drug Release of Homogeneously Distributed Chitosan Nanoparticles with a High Encapsulation Efficiency. *Fibers Polym.* **2020**, *21*, 1917–1926. [[CrossRef](#)]
47. Xun, X.-M.; Zhang, Z.-A.; Yuan, Z.-X.; Tuhong, K.; Yan, C.-H.; Zhan, Y.-F.; Kang, G.-P.; Wu, Q.-Y.; Wang, J. Novel Caffeic Acid Grafted Chitosan-Sodium Alginate Microcapsules Generated by Microfluidic Technique for the Encapsulation of Bioactive Peptides from Silkworm Pupae. *Sustain. Chem. Pharm.* **2023**, *32*, 100974. [[CrossRef](#)]
48. Park, J.W.; Park, K.H.; Seo, S. Natural Polyelectrolyte Complex-based PH-dependent Delivery Carriers Using Alginate and Chitosan. *J. Appl. Polym. Sci.* **2019**, *136*, 48143. [[CrossRef](#)]
49. Nazlı, A.B.; Açikel, Y.S. Loading of Cancer Drug Resveratrol to PH-Sensitive, Smart, Alginate-Chitosan Hydrogels and Investigation of Controlled Release Kinetics. *J. Drug Deliv. Sci. Technol.* **2019**, *53*, 101199. [[CrossRef](#)]
50. Zeng, W.; Liu, Z.; Li, Y.; Zhu, S.; Ma, J.; Li, W.; Gao, G. Development and Characterization of Cores-Shell Poly(Lactide-Co-Glycolide)-Chitosan Microparticles for Sustained Release of GDNF. *Colloids Surf. B Biointerfaces* **2017**, *159*, 791–799. [[CrossRef](#)]
51. Higuera-Ciapara, I.; Felix-Valenzuela, L.; Goycoolea, F.M.; Argüelles-Monal, W. Microencapsulation of Astaxanthin in a Chitosan Matrix. *Carbohydr. Polym.* **2004**, *56*, 41–45. [[CrossRef](#)]
52. Huang, W.F.; Tsui, C.P.; Tang, C.Y.; Yang, M.; Gu, L. Surface Charge Switchable and PH-Responsive Chitosan/Polymer Core-Shell Composite Nanoparticles for Drug Delivery Application. *Compos. Part B Eng.* **2017**, *121*, 83–91. [[CrossRef](#)]
53. Dozie-Nwachukwu, S.O.; Danyuo, Y.; Obayemi, J.D.; Odusanya, O.S.; Malatesta, K.; Soboyejo, W.O. Extraction and Encapsulation of Prodigiosin in Chitosan Microspheres for Targeted Drug Delivery. *Mater. Sci. Eng. C* **2017**, *71*, 268–278. [[CrossRef](#)] [[PubMed](#)]
54. Budincic, J.M.; Petrovic, L.; Dekic, L.; Fraj, J.; Bucko, S.; Katona, J.; Spasojevic, L. Study of Vitamin E Microencapsulation and Controlled Release from Chitosan/Sodium Lauryl Ether Sulfate Microcapsules. *Carbohydr. Polym.* **2021**, *251*, 116988. [[CrossRef](#)]
55. Kurakula, M.; Raghavendra Naveen, N. Electrospinning: A Facile Technology Unfolding the Chitosan Based Drug Delivery and Biomedical Applications. *Eur. Polym. J.* **2021**, *147*, 110326. [[CrossRef](#)]
56. Hijazi, N.; Rodier, E.; Letourneau, J.-J.; Louati, H.; Sauceau, M.; Le Moigne, N.; Benezet, J.-C.; Fages, J. Chitosan Nanoparticles Generation Using CO₂ Assisted Processes. *J. Supercrit. Fluids* **2014**, *95*, 118–128. [[CrossRef](#)]
57. Nguyen, D.T.; Phan, V.H.G.; Lee, D.S.; Thambi, T.; Huynh, D.P. Bioresorbable PH- and Temperature-Responsive Injectable Hydrogels-Incorporating Electrospayed Particles for the Sustained Release of Insulin. *Polym. Degrad. Stab.* **2019**, *162*, 36–46. [[CrossRef](#)]
58. Hiroyuki, T.; Hideki, I.; Yoshinobu, F. Chitosan-Gadopentetic Acid Complex Nanoparticles for Gadolinium Neutron-Capture Therapy of Cancer: Preparation by Novel Emulsion-Droplet Coalescence Technique and Characterization. *Pharm. Res.* **1999**, *16*, 1830–1835. [[CrossRef](#)]
59. Sheikholeslami, Z.S.; Salimi-Kenari, H.; Imani, M.; Atai, M.; Nodehi, A. Exploring the Effect of Formulation Parameters on the Particle Size of Carboxymethyl Chitosan Nanoparticles Prepared via Reverse Micellar Crosslinking. *J. Microencapsul.* **2017**, *34*, 270–279. [[CrossRef](#)]
60. Mitra, S.; Gaur, U.; Ghosh, P.C.; Maitra, A.N. Tumour Targeted Delivery of Encapsulated Dextran-Doxorubicin Conjugate Using Chitosan Nanoparticles as Carrier. *J. Control. Release* **2001**, *74*, 317–323. [[CrossRef](#)]
61. Agnihotri, S.A.; Aminabhavi, T.M. Controlled Release of Clozapine through Chitosan Microparticles Prepared by a Novel Method. *J. Control. Release* **2004**, *96*, 245–259. [[CrossRef](#)]
62. Bellich, B.; D’Agostino, I.; Semeraro, S.; Gamini, A.; Cesàro, A. “The Good, the Bad and the Ugly” of Chitosans. *Mar. Drugs* **2016**, *14*, 99. [[CrossRef](#)]

63. Siepmann, J.; Siepmann, F. Mathematical Modeling of Drug Delivery. *Int. J. Pharm.* **2008**, *364*, 328–343. [[CrossRef](#)]
64. Abdel-Hafez, S.M.; Hathout, R.M.; Sammour, O.A. Towards Better Modeling of Chitosan Nanoparticles Production: Screening Different Factors and Comparing Two Experimental Designs. *Int. J. Biol. Macromol.* **2014**, *64*, 334–340. [[CrossRef](#)]
65. Sreekumar, S.; Goycoolea, F.M.; Moerschbacher, B.M.; Rivera-Rodriguez, G.R. Parameters Influencing the Size of Chitosan-TPP Nano- and Microparticles. *Sci. Rep.* **2018**, *8*, 4695. [[CrossRef](#)]
66. Thakur, A.; Taranjit. Preparation of Chitosan Nanoparticles: A Study of Influencing Factors. In Proceedings of the International Conference On Advances in Condensed And Nano Materials (ICACNM-2011), Chandigarh, India, 23–26 February 2011; AIP Conference Proceedings: College Park, MD, USA, 2011; pp. 299–300.
67. Martins, E.; Poncellet, D.; Rodrigues, R.C.; Renard, D. Oil Encapsulation Techniques Using Alginate as Encapsulating Agent: Applications and Drawbacks. *J. Microencapsul.* **2017**, *34*, 754–771. [[CrossRef](#)]
68. Lee, Y.; Ji, Y.R.; Lee, S.; Choi, M.-J.; Cho, Y. Microencapsulation of Probiotic *Lactobacillus Acidophilus* KBL409 by Extrusion Technology to Enhance Survival under Simulated Intestinal and Freeze-Drying Conditions. *J. Microbiol. Biotechnol.* **2019**, *29*, 721–730. [[CrossRef](#)]
69. Calvo, P.; Remuñán-López, C.; Vila-Jato, J.L.; Alonso, M.J. Novel Hydrophilic Chitosan-Polyethylene Oxide Nanoparticles as Protein Carriers. *J. Appl. Polym. Sci.* **1997**, *63*, 125–132. [[CrossRef](#)]
70. Fan, W.; Yan, W.; Xu, Z.; Ni, H. Formation Mechanism of Monodisperse, Low Molecular Weight Chitosan Nanoparticles by Ionic Gelation Technique. *Colloids Surf. B Biointerfaces* **2012**, *90*, 21–27. [[CrossRef](#)]
71. Hasheminejad, N.; Khodaiyan, F.; Safari, M. Improving the Antifungal Activity of Clove Essential Oil Encapsulated by Chitosan Nanoparticles. *Food Chem.* **2019**, *275*, 113–122. [[CrossRef](#)]
72. Nair, R.S.; Morris, A.; Billa, N.; Leong, C.-O. An Evaluation of Curcumin-Encapsulated Chitosan Nanoparticles for Transdermal Delivery. *AAPS PharmSciTech* **2019**, *20*, 69. [[CrossRef](#)] [[PubMed](#)]
73. Phan, A.N.Q.; Bach, L.G.; Nguyen, T.D.; Le, N.T.H. Efficient Method for Preparation of Rutin Nanosuspension Using Chitosan and Sodium Tripolyphosphate Crosslinker. *J. Nanosci. Nanotechnol.* **2019**, *19*, 974–978. [[CrossRef](#)] [[PubMed](#)]
74. Bin-Jumah, M.; Gilani, S.J.; Jahangir, M.A.; Zafar, A.; Alshehri, S.; Yasir, M.; Kala, C.; Taleuzzaman, M.; Imam, S.S. Clarithromycin-Loaded Ocular Chitosan Nanoparticle: Formulation, Optimization, Characterization, Ocular Irritation, and Antimicrobial Activity. Available online: <https://www.dovepress.com/clarithromycin-loaded-ocular-chitosan-nanoparticle-formulation-optimiz-peer-reviewed-fulltext-article-IJN> (accessed on 15 January 2021).
75. Das, S.; Singh, V.K.; Dwivedy, A.K.; Chaudhari, A.K.; Upadhyay, N.; Singh, P.; Sharma, S.; Dubey, N.K. Encapsulation in Chitosan-Based Nanomatrix as an Efficient Green Technology to Boost the Antimicrobial, Antioxidant and in Situ Efficacy of *Coriandrum Sativum* Essential Oil. *Int. J. Biol. Macromol.* **2019**, *133*, 294–305. [[CrossRef](#)] [[PubMed](#)]
76. Hu, Y.; Jiang, X.; Ding, Y.; Ge, H.; Yuan, Y.; Yang, C. Synthesis and Characterization of Chitosan–Poly(Acrylic Acid) Nanoparticles. *Biomaterials* **2002**, *23*, 3193–3201. [[CrossRef](#)] [[PubMed](#)]
77. Li, X.; Kong, X.; Shi, S.; Zheng, X.; Guo, G.; Wei, Y.; Qian, Z. Preparation of Alginate Coated Chitosan Microparticles for Vaccine Delivery. *BMC Biotechnol.* **2008**, *8*, 89. [[CrossRef](#)]
78. Liu, F.; Liu, L.; Li, X.; Zhang, Q. Preparation of Chitosan–Hyaluronate Double-Walled Microspheres by Emulsification-Coacervation Method. *J. Mater. Sci. Mater. Med.* **2007**, *18*, 2215–2224. [[CrossRef](#)]
79. Rathore, P. Formulation Development, in Vitro and in Vivo Evaluation of Chitosan Engineered Nanoparticles for Ocular Delivery of Insulin. *RSC Adv.* **2020**, *10*, 43629–43639. [[CrossRef](#)]
80. Saraf, S.; Jain, S.; Sahoo, R.N.; Mallick, S. Lipopolysaccharide Derived Alginate Coated Hepatitis B Antigen Loaded Chitosan Nanoparticles for Oral Mucosal Immunization. *Int. J. Biol. Macromol.* **2020**, *154*, 466–476. [[CrossRef](#)]
81. Zhang, W.; Jin, X.; Li, H.; Wei, C.; Wu, C. Onion-Structure Bionic Hydrogel Capsules Based on Chitosan for Regulating Doxorubicin Release. *Carbohydr. Polym.* **2019**, *209*, 152–160. [[CrossRef](#)]
82. Rodkate, N.; Rutnakornpituk, M. Multi-Responsive Magnetic Microsphere of Poly(N-Isopropylacrylamide)/Carboxymethylchitosan Hydrogel for Drug Controlled Release. *Carbohydr. Polym.* **2016**, *151*, 251–259. [[CrossRef](#)]
83. Maity, S.; Mukhopadhyay, P.; Kundu, P.P.; Chakraborti, A.S. Alginate Coated Chitosan Core-Shell Nanoparticles for Efficient Oral Delivery of Naringenin in Diabetic Animals—An in Vitro and in Vivo Approach. *Carbohydr. Polym.* **2017**, *170*, 124–132. [[CrossRef](#)]
84. Soe, Z.C.; Poudel, B.K.; Nguyen, H.T.; Thapa, R.K.; Ou, W.; Gautam, M.; Poudel, K.; Jin, S.G.; Jeong, J.-H.; Ku, S.K.; et al. Folate-Targeted Nanostructured Chitosan/Chondroitin Sulfate Complex Carriers for Enhanced Delivery of Bortezomib to Colorectal Cancer Cells. *Asian J. Pharm. Sci.* **2019**, *14*, 40–51. [[CrossRef](#)]
85. Chaiyasan, W.; Srinivas, S.P.; Tiyaboonchai, W. Crosslinked Chitosan-Dextran Sulfate Nanoparticle for Improved Topical Ocular Drug Delivery. *Mol. Vis.* **2015**, *21*, 1224–1234.
86. Mukhopadhyay, P.; Chakraborty, S.; Bhattacharya, S.; Mishra, R.; Kundu, P.P. PH-Sensitive Chitosan/Alginate Core-Shell Nanoparticles for Efficient and Safe Oral Insulin Delivery. *Int. J. Biol. Macromol.* **2015**, *72*, 640–648. [[CrossRef](#)]
87. Özbaş-Turan, S.; Akbuğa, J.; Aral, C. Controlled Release of Interleukin-2 from Chitosan Microspheres. *J. Pharm. Sci.* **2002**, *91*, 1245–1251. [[CrossRef](#)]
88. Kumar, A.; Gupta, V.; Singh, P.P.; Kujur, A.; Prakash, B. Fabrication of Volatile Compounds Loaded-Chitosan Biopolymer Nanoparticles: Optimization, Characterization and Assessment against *Aspergillus Flavus* and Aflatoxin B1 Contamination. *Int. J. Biol. Macromol.* **2020**, *165*, 1507–1518. [[CrossRef](#)]

89. Lam, P.-L.; Lee, K.K.-H.; Ho, Y.-W.; Wong, R.S.-M.; Tong, S.-W.; Cheng, C.-H.; Lam, K.-H.; Tang, J.C.-O.; Bian, Z.-X.; Gambari, R.; et al. The Development of Chitosan Based Microcapsules as Delivery Vehicles for Orally Administered Daunorubicin. *RSC Adv.* **2014**, *4*, 14109–14114. [[CrossRef](#)]
90. Lim, L.Y.; Wan, L.S.C.; Thai, P.Y. Chitosan Microspheres Prepared by Emulsification and Ionotropic Gelation. *Drug Dev. Ind. Pharm.* **1997**, *23*, 981–985. [[CrossRef](#)]
91. Biró, E.; Németh, A.S.; Feczko, T.; Tóth, J.; Sisak, C.; Gyenis, J. Three-Step Experimental Design to Determine the Effect of Process Parameters on the Size of Chitosan Microspheres. *Chem. Eng. Process. Process Intensif.* **2009**, *48*, 771–779. [[CrossRef](#)]
92. Patil, S.B.; Sawant, K.K. Chitosan Microspheres as a Delivery System for Nasal Insufflation. *Colloids Surf. B Biointerfaces* **2011**, *84*, 384–389. [[CrossRef](#)]
93. Dhawan, S.; Singla, A.K.; Sinha, V.R. Evaluation of Mucoadhesive Properties of Chitosan Microspheres Prepared by Different Methods. *AAPS PharmSciTech* **2004**, *5*, 122–128. [[CrossRef](#)] [[PubMed](#)]
94. Nayak, U.Y.; Gopal, S.; Mutalik, S.; Ranjith, A.K.; Reddy, M.S.; Gupta, P.; Udupa, N. Glutaraldehyde Cross-Linked Chitosan Microspheres for Controlled Delivery of Zidovudine. *J. Microencapsul.* **2009**, *26*, 214–222. [[CrossRef](#)] [[PubMed](#)]
95. Abulaihaiti, M.; Wu, X.-W.; Qiao, L.; Lv, H.-L.; Zhang, H.-W.; Aduwayi, N.; Wang, Y.-J.; Wang, X.-C.; Peng, X.-Y. Efficacy of Albendazole-Chitosan Microsphere-Based Treatment for Alveolar Echinococcosis in Mice. *PLoS Negl. Trop. Dis.* **2015**, *9*, e0003950. [[CrossRef](#)] [[PubMed](#)]
96. El-Shabouri, M.H. Positively Charged Nanoparticles for Improving the Oral Bioavailability of Cyclosporin-A. *Int. J. Pharm.* **2002**, *249*, 101–108. [[CrossRef](#)]
97. Niwa, T.; Takeuchi, H.; Hino, T.; Kunou, N.; Kawashima, Y. Preparations of Biodegradable Nanospheres of Water-Soluble and Insoluble Drugs with D,L-Lactide/Glycolide Copolymer by a Novel Spontaneous Emulsification Solvent Diffusion Method, and the Drug Release Behavior. *J. Control. Release* **1993**, *25*, 89–98. [[CrossRef](#)]
98. Liu, W.; Wu, W.D.; Selomulya, C.; Chen, X.D. Uniform Chitosan Microparticles Prepared by a Novel Spray-Drying Technique. *Int. J. Chem. Eng.* **2011**, *2011*, 267218. [[CrossRef](#)]
99. Ngan, L.T.K.; Wang, S.-L.; Hiep, Đ.M.; Luong, P.M.; Vui, N.T.; Đinh, T.M.; Dzung, N.A. Preparation of Chitosan Nanoparticles by Spray Drying, and Their Antibacterial Activity. *Res. Chem. Intermed.* **2014**, *40*, 2165–2175. [[CrossRef](#)]
100. Acosta, N.; Sánchez, E.; Calderón, L.; Córdoba-Díaz, M.; Córdoba-Díaz, D.; Dom, S.; Heras, Á. Physical Stability Studies of Semi-Solid Formulations from Natural Compounds Loaded with Chitosan Microspheres. *Mar. Drugs* **2015**, *13*, 5901–5919. [[CrossRef](#)]
101. Aranaz, I.; Paños, I.; Peniche, C.; Heras, Á.; Acosta, N. Chitosan Spray-Dried Microparticles for Controlled Delivery of Venlafaxine Hydrochloride. *Molecules* **2017**, *22*, 1980. [[CrossRef](#)]
102. Khlibsuwan, R.; Siepmann, F.; Siepmann, J.; Pongjanyakul, T. Chitosan-Clay Nanocomposite Microparticles for Controlled Drug Delivery: Effects of the MAS Content and TPP Crosslinking. *J. Drug Deliv. Sci. Technol.* **2017**, *40*, 1–10. [[CrossRef](#)]
103. Amidi, M.; Pellikaan, H.C.; de Boer, A.H.; Crommelin, D.J.A.; Hennink, W.E.; Jiskoot, W. Preparation and Physicochemical Characterization of Supercritically Dried Insulin-Loaded Microparticles for Pulmonary Delivery. *Eur. J. Pharm. Biopharm.* **2008**, *68*, 191–200. [[CrossRef](#)]
104. Moreno, J.A.S.; Mendes, A.C.; Stephansen, K.; Engwer, C.; Goycoolea, F.M.; Boisen, A.; Nielsen, L.H.; Chronakis, I.S. Development of Electrospayed Mucoadhesive Chitosan Microparticles. *Carbohydr. Polym.* **2018**, *190*, 240–247. [[CrossRef](#)]
105. Sreekumar, S.; Lemke, P.; Moerschbacher, B.M.; Torres-Giner, S.; Lagaron, J.M. Preparation and Optimization of Submicron Chitosan Capsules by Water-Based Electrospaying for Food and Bioactive Packaging Applications. *Food Addit. Contam. Part A* **2017**, *34*, 1795–1806. [[CrossRef](#)]
106. Cui, C.; Gan, L.; Lan, X.; Li, J.; Zhang, C.; Li, F.; Wang, C.; Yuan, C. Development of Sustainable Carrier in Thermosensitive Hydrogel Based on Chitosan/Alginate Nanoparticles for *in Situ* Delivery System. *Polym. Compos.* **2019**, *40*, 2187–2196. [[CrossRef](#)]
107. Calvo, P.; Remuñán-López, C.; Vila-Jato, J.L.; Alonso, M.J. Development of Positively Charged Colloidal Drug Carriers: Chitosan-Coated Polyester Nanocapsules and Submicron-Emulsions. *Colloid Polym. Sci.* **1997**, *275*, 46–53. [[CrossRef](#)]
108. Hoffmann, S.; Gorzelanny, C.; Moerschbacher, B.; Goycoolea, F. Physicochemical Characterization of FRET-Labelled Chitosan Nanocapsules and Model Degradation Studies. *Nanomaterials* **2018**, *8*, 846. [[CrossRef](#)]
109. Prego, C.; Fabre, M.; Torres, D.; Alonso, M.J. Efficacy and Mechanism of Action of Chitosan Nanocapsules for Oral Peptide Delivery. *Pharm. Res.* **2006**, *23*, 549–556. [[CrossRef](#)]
110. Yang, X.-L.; Ju, X.-J.; Mu, X.-T.; Wang, W.; Xie, R.; Liu, Z.; Chu, L.-Y. Core-Shell Chitosan Microcapsules for Programmed Sequential Drug Release. *ACS Appl. Mater. Interfaces* **2016**, *8*, 10524–10534. [[CrossRef](#)]
111. Huang, K.-S.; Yang, C.-H.; Wang, Y.-C.; Wang, W.-T.; Lu, Y.-Y. Microfluidic Synthesis of Vinblastine-Loaded Multifunctional Particles for Magnetically Responsive Controlled Drug Release. *Pharmaceutics* **2019**, *11*, 212. [[CrossRef](#)]
112. Mou, C.-L.; Wang, W.; Ju, X.-J.; Xie, R.; Liu, Z.; Chu, L.-Y. Dual-Responsive Microcarriers with Sphere-in-Capsule Structures for Co-Encapsulation and Sequential Release. *J. Taiwan Inst. Chem. Eng.* **2019**, *98*, 63–69. [[CrossRef](#)]
113. Ling, K.; Wu, H.; Neish, A.S.; Champion, J.A. Alginate/Chitosan Microparticles for Gastric Passage and Intestinal Release of Therapeutic Protein Nanoparticles. *J. Control. Release* **2019**, *295*, 174–186. [[CrossRef](#)] [[PubMed](#)]
114. He, X.-H.; Wang, W.; Deng, K.; Xie, R.; Ju, X.-J.; Liu, Z.; Chu, L.-Y. Microfluidic Fabrication of Chitosan Microfibers with Controllable Internals from Tubular to Peapod-like Structures. *RSC Adv.* **2015**, *5*, 928–936. [[CrossRef](#)]

115. Rao, A.; Schoenenberger, M.; Gnecco, E.; Glatzel, T.; Meyer, E.; Brändlin, D.; Scandella, L. Characterization of Nanoparticles Using Atomic Force Microscopy. *J. Phys. Conf. Ser.* **2007**, *61*, 971. [[CrossRef](#)]
116. Otlés, S.; Ozyurt, V.H. Electron Microscopy Techniques. In *Microstructure of Dairy Products*; John Wiley & Sons: Hoboken, NJ, USA, 2018; pp. 51–66.
117. Pei, Y.; Hinchliffe, B.A.; Minelli, C. Measurement of the Size Distribution of Multimodal Colloidal Systems by Laser Diffraction. *ACS Omega* **2021**, *6*, 14049–14058. [[CrossRef](#)]
118. Berne, B.J.; Pecora, R. *Dynamic Light Scattering: With Applications to Chemistry, Biology, and Physics*; Courier Corporation: Chelmsford, MA, USA, 2000.
119. Agarwal, R.; Journey, P.; Raythatha, M.; Singh, V.; Sreenivasan, S.V.; Shi, L.; Roy, K. Effect of Shape, Size, and Aspect Ratio on Nanoparticle Penetration and Distribution inside Solid Tissues Using 3D Spheroid Models. *Adv. Healthc. Mater.* **2015**, *4*, 2269–2280. [[CrossRef](#)]
120. Geng, Y.; Dalhaimer, P.; Cai, S.; Tsai, R.; Tewari, M.; Minko, T.; Discher, D.E. Shape Effects of Filaments versus Spherical Particles in Flow and Drug Delivery. *Nat. Nanotechnol.* **2007**, *2*, 249–255. [[CrossRef](#)]
121. Boulanger, G.; Andujar, P.; Paireon, J.-C.; Billon-Galland, M.-A.; Dion, C.; Dumortier, P.; Brochard, P.; Sobaszek, A.; Bartsch, P.; Paris, C.; et al. Quantification of Short and Long Asbestos Fibers to Assess Asbestos Exposure: A Review of Fiber Size Toxicity. *Environ. Health* **2014**, *13*, 59. [[CrossRef](#)]
122. Chandra, J.; George, N.; Narayanankutty, S.K. Isolation and Characterization of Cellulose Nanofibrils from Arecanut Husk Fibre. *Carbohydr. Polym.* **2016**, *142*, 158–166. [[CrossRef](#)]
123. Ouf, F.-X.; Bourrous, S.; Vallières, C.; Yon, J.; Lintis, L. Specific Surface Area of Combustion Emitted Particles: Impact of Primary Particle Diameter and Organic Content. *J. Aerosol Sci.* **2019**, *137*, 105436. [[CrossRef](#)]
124. Li, T.; Senesi, A.J.; Lee, B. Small Angle X-Ray Scattering for Nanoparticle Research. *Chem. Rev.* **2016**, *116*, 11128–11180. [[CrossRef](#)]
125. Svergun, D.I.; Koch, M.H.J. Small-Angle Scattering Studies of Biological Macromolecules in Solution. *Rep. Prog. Phys.* **2003**, *66*, 1735. [[CrossRef](#)]
126. Klose, D.; Siepmann, F.; Elkharraz, K.; Krenzlin, S.; Siepmann, J. How Porosity and Size Affect the Drug Release Mechanisms from PLGA-Based Microparticles. *Int. J. Pharm.* **2006**, *314*, 198–206. [[CrossRef](#)]
127. Mi, F.-L.; Lin, Y.-M.; Wu, Y.-B.; Shyu, S.-S.; Tsai, Y.-H. Chitin/PLGA Blend Microspheres as a Biodegradable Drug-Delivery System: Phase-Separation, Degradation and Release Behavior. *Biomaterials* **2002**, *23*, 3257–3267. [[CrossRef](#)]
128. Mukhopadhyay, P.; Kundu, P.P. Chitosan-Graft-PAMAM–Alginate Core–Shell Nanoparticles: A Safe and Promising Oral Insulin Carrier in an Animal Model. *RSC Adv.* **2015**, *5*, 93995–94007. [[CrossRef](#)]
129. Yang, X.; Lu, Y. Hollow Nanometer-Sized Polypyrrole Capsules with Controllable Shell Thickness Synthesized in the Presence of Chitosan. *Polymer* **2005**, *46*, 5324–5328. [[CrossRef](#)]
130. Lamprecht, A.; Schäfer, U.F.; Lehr, C.-M. Characterization of Microcapsules by Confocal Laser Scanning Microscopy: Structure, Capsule Wall Composition and Encapsulation Rate. *Eur. J. Pharm. Biopharm.* **2000**, *49*, 1–9. [[CrossRef](#)]
131. Liu, C.; Pei, R.; Peltonen, L.; Heinonen, M. Assembling of the Interfacial Layer Affects the Physical and Oxidative Stability of Faba Bean Protein-Stabilized Oil-in-Water Emulsions with Chitosan. *Food Hydrocoll.* **2020**, *102*, 105614. [[CrossRef](#)]
132. Han, Y.; Tong, W.; Zhang, Y.; Gao, C. Fabrication of Chitosan Single-Component Microcapsules With a Micrometer-Thick and Layered Wall Structure by Stepwise Core-Mediated Precipitation. *Macromol. Rapid Commun.* **2012**, *33*, 326–331. [[CrossRef](#)]
133. Arzumanyan, G.; Linnik, D.; Mamatkulov, K.; Vorobyeva, M.; Korsun, A.; Glasunova, V.; Jevremović, A. Synthesis of NaYF₄:Yb,Er@SiO₂@Ag Core-Shell Nanoparticles for Plasmon-Enhanced Upconversion Luminescence in Bio-Applications. *Ann. Biomed. Sci. Eng.* **2019**, *3*, 013–019. [[CrossRef](#)]
134. Grassi, M.; Grassi, G. Mathematical Modelling and Controlled Drug Delivery: Matrix Systems. *Curr. Drug Deliv.* **2005**, *2*, 97–116. [[CrossRef](#)]
135. Feng, S.-S.; Ruan, G.; Li, Q.-T. Fabrication and Characterizations of a Novel Drug Delivery Device Liposomes-in-Microsphere (LIM). *Biomaterials* **2004**, *25*, 5181–5189. [[CrossRef](#)] [[PubMed](#)]
136. Lu, C.; Mu, B.; Liu, P. Stimuli-Responsive Multilayer Chitosan Hollow Microspheres via Layer-by-Layer Assembly. *Colloids Surf. B Biointerfaces* **2011**, *83*, 254–259. [[CrossRef](#)] [[PubMed](#)]
137. Niu, S.; Williams, G.R.; Wu, J.; Wu, J.; Zhang, X.; Zheng, H.; Li, S.; Zhu, L.-M. A Novel Chitosan-Based Nanomedicine for Multi-Drug Resistant Breast Cancer Therapy. *Chem. Eng. J.* **2019**, *369*, 134–149. [[CrossRef](#)]
138. Herdiana, Y.; Wathoni, N.; Shamsuddin, S.; Muchtaridi, M. Drug Release Study of the Chitosan-Based Nanoparticles. *Heliyon* **2022**, *8*, e08674. [[CrossRef](#)]
139. Wagner, J.G. Interpretation of Percent Dissolved-Time Plots Derived from In Vitro Testing of Conventional Tablets and Capsules. *J. Pharm. Sci.* **1969**, *58*, 1253–1257. [[CrossRef](#)]
140. Gibaldi, M.; Feldman, S. Establishment of Sink Conditions in Dissolution Rate Determinations. Theoretical Considerations and Application to Nondisintegrating Dosage Forms. *J. Pharm. Sci.* **1967**, *56*, 1238–1242. [[CrossRef](#)]
141. Higuchi, T. Mechanism of Sustained-Action Medication. Theoretical Analysis of Rate of Release of Solid Drugs Dispersed in Solid Matrices. *J. Pharm. Sci.* **1963**, *52*, 1145–1149. [[CrossRef](#)]
142. Korsmeyer, R.W.; Gurny, R.; Doelker, E.; Buri, P.; Peppas, N.A. Mechanisms of Solute Release from Porous Hydrophilic Polymers. *Int. J. Pharm.* **1983**, *15*, 25–35. [[CrossRef](#)]
143. Bruschi, M.L. *Strategies to Modify the Drug Release from Pharmaceutical Systems*; Woodhead Publishing: Cambridge, UK, 2015.

144. Kosmidis, K.; Argyrakis, P.; Macheras, P. Fractal Kinetics in Drug Release from Finite Fractal Matrices. *J. Chem. Phys.* **2003**, *119*, 6373–6377. [[CrossRef](#)]
145. Hixson, A.W.; Crowell, J.H. Dependence of Reaction Velocity upon Surface and Agitation. *Ind. Eng. Chem.* **1931**, *23*, 923–931. [[CrossRef](#)]
146. Peppas, N.A.; Sahlin, J.J. A Simple Equation for the Description of Solute Release. III. Coupling of Diffusion and Relaxation. *Int. J. Pharm.* **1989**, *57*, 169–172. [[CrossRef](#)]
147. Kopcha, M.; Lordi, N.G.; Tojo, K.J. Evaluation of Release from Selected Thermosoftening Vehicles. *J. Pharm. Pharmacol.* **1991**, *43*, 382–387. [[CrossRef](#)]
148. Baker, R.; Lonsdale, H. Controlled Release: Mechanisms and Rates. *Control. Release Biol. Act. Agents* **1974**, *15*.
149. Shukla, A.J.; Price, J.C. Effect of Drug (Core) Particle Size on the Dissolution of Theophylline from Microspheres Made from Low Molecular Weight Cellulose Acetate Propionate. *Pharm. Res.* **1989**, *6*, 418–421. [[CrossRef](#)]
150. Shukla, A.J.; Price, J.C. Effect of Drug Loading and Molecular Weight of Cellulose Acetate Propionate on the Release Characteristics of Theophylline Microspheres. *Pharm. Res.* **1991**, *8*, 1396–1400. [[CrossRef](#)] [[PubMed](#)]
151. Hopfenberg, H.B. Controlled Release from Erodible Slabs, Cylinders, and Spheres. In *Controlled Release Polymeric Formulations*; ACS Symposium Series; American Chemical Society: Washington, DC, USA, 1976; Volume 33, pp. 26–32, ISBN 978-0-8412-0341-9.
152. Tsigotis-Maniecka, M.; Szyk-Warszyńska, L.; Maniecki, L.; Szczesna, W.; Warszyński, P.; Wilk, K.A. Tailoring the Composition of Hydrogel Particles for the Controlled Delivery of Phytopharmaceuticals. *Eur. Polym. J.* **2021**, *151*, 110429. [[CrossRef](#)]
153. Bugatti, V.; Vertuccio, L.; Zara, S.; Fancello, F.; Scanu, B.; Gorrasi, G. Green Pesticides Based on Cinnamate Anion Incorporated in Layered Double Hydroxides and Dispersed in Pectin Matrix. *Carbohydr. Polym.* **2019**, *209*, 356–362. [[CrossRef](#)] [[PubMed](#)]
154. Jardim, K.V.; Palomec-Garfias, A.F.; Araújo, M.V.; Márquez-Beltrán, C.; Bakuzis, A.F.; Moya, S.E.; Parize, A.L.; Sousa, M.H. Remotely Triggered Curcumin Release from Stimuli-Responsive Magneto-Polymeric Layer-by-Layer Engineered Nanoplatfoms. *J. Appl. Polym. Sci.* **2022**, *139*, 52200. [[CrossRef](#)]
155. Liu, C.; Desai, K.G.H.; Tang, X.; Chen, X. Drug Release Kinetics of Spray-Dried Chitosan Microspheres. *Dry. Technol.* **2006**, *24*, 769–776. [[CrossRef](#)]
156. Dahan, W.M.; Mohammad, F.; Ezzat, A.O.; Atta, A.M.; Al-Tilasi, H.H.; Al-Lohedan, H.A. Influence of Amidation on the Release Profiles of Insulin Drug from Chitosan-Based Matrices. *Coatings* **2022**, *12*, 465. [[CrossRef](#)]
157. Thai, H.; Thuy Nguyen, C.; Thi Thach, L.; Thi Tran, M.; Duc Mai, H.; Thi Thu Nguyen, T.; Duc Le, G.; Van Can, M.; Dai Tran, L.; Long Bach, G.; et al. Characterization of Chitosan/Alginate/Lovastatin Nanoparticles and Investigation of Their Toxic Effects in Vitro and in Vivo. *Sci. Rep.* **2020**, *10*, 909. [[CrossRef](#)]
158. Whitehead, F.A.; Kasapis, S. Modelling the Mechanism and Kinetics of Ascorbic Acid Diffusion in Genipin-Crosslinked Gelatin and Chitosan Networks at Distinct PH. *Food Biosci.* **2022**, *46*, 101579. [[CrossRef](#)]
159. Tapia, C.; Escobar, Z.; Costa, E.; Sapag-Hagar, J.; Valenzuela, F.; Basualto, C.; Nella Gai, M.; Yazdani-Pedram, M. Comparative Studies on Polyelectrolyte Complexes and Mixtures of Chitosan–Alginate and Chitosan–Carrageenan as Prolonged Diltiazem Chlorhydrate Release Systems. *Eur. J. Pharm. Biopharm.* **2004**, *57*, 65–75. [[CrossRef](#)]
160. Liu, H.; Gong, L.; Lu, S.; Wang, H.; Fan, W.; Yang, C. Three Core-Shell Polymersomes for Targeted Doxorubicin Delivery: Sustained and Acidic Release. *J. Drug Deliv. Sci. Technol.* **2021**, *61*, 102293. [[CrossRef](#)]
161. Yan, S.; Rao, S.; Zhu, J.; Wang, Z.; Zhang, Y.; Duan, Y.; Chen, X.; Yin, J. Nanoporous Multilayer Poly(L-Glutamic Acid)/Chitosan Microcapsules for Drug Delivery. *Int. J. Pharm.* **2012**, *427*, 443–451. [[CrossRef](#)]
162. Zhou, Y.; Chu, J.S.; Wu, X.Y. Theoretical Analysis of Drug Release into a Finite Medium from Sphere Ensembles with Various Size and Concentration Distributions. *Eur. J. Pharm. Sci.* **2004**, *22*, 251–259. [[CrossRef](#)]
163. Spiridonova, T.I.; Tverdokhlebov, S.I.; Anissimov, Y.G. Investigation of the Size Distribution for Diffusion-Controlled Drug Release From Drug Delivery Systems of Various Geometries. *J. Pharm. Sci.* **2019**, *108*, 2690–2697. [[CrossRef](#)]
164. Teimouri, S.; Dekiwadia, C.; Kasapis, S. Decoupling Diffusion and Macromolecular Relaxation in the Release of Vitamin B6 from Genipin-Crosslinked Whey Protein Networks. *Food Chem.* **2021**, *346*, 128886. [[CrossRef](#)]

Disclaimer/Publisher’s Note: The statements, opinions and data contained in all publications are solely those of the individual author(s) and contributor(s) and not of MDPI and/or the editor(s). MDPI and/or the editor(s) disclaim responsibility for any injury to people or property resulting from any ideas, methods, instructions or products referred to in the content.